THE DISTRIBUTION OF MICROPLASTICS IN MARSHLANDS SURROUNDED BY AGRICULTURE FIELDS - ELKHORN SLOUGH, CA

A Thesis

Presented to the

Faculty of

Moss Landing Marine Laboratories

California State University Monterey Bay

In Partial Fulfillment

of the Requirements for the Degree

Master of Science

in

Marine Science

---

by

Victoria Dickey

Fall 2022

Copyright © 2022

by

Victoria Dickey

All Rights Reserved

DocuSign Envelope ID: F0064617-D3D8-4E2B-9F49-09310BC7BC6F

CALIFORNIA STATE UNIVERSITY MONTEREY BAY

The Undersigned Faculty Committee Approves the

Thesis of Victoria Dickey:

THE DISTRIBUTION OF MICROPLASTICS IN MARSHLANDS

SURROUNDED BY AGRICULTURE FIELDS- ELKHORN SLOUGH, CA

DocuSigned by:
Ivano Aiello
10434850E8C446C...

Ivano Aiello
Chair
Moss Landing Marine Laboratories

DocuSigned by:
Maxime Grand
B182CE7C19BE48D...

Maxime Grand
Moss Landing Marine Laboratories

DocuSigned by:
Emily Miller
4A88C0F593B44FB...

Emily Miller
Monterey Bay Aquarium

Doug Smith

Doug Smith
CSUMB Interim Dean of Graduate Studies & Research

12/18/2022

Approval Date

DEDICATION

I dedicate this thesis to my family in San Diego and the family of friends I have gained in Monterey. Thank you all so much for your unwavering support.

ABSTRACT

The distribution of microplastics in marshlands surrounded by
agriculture fields- Elkhorn Slough, CA

by
Victoria Dickey
Master of Science in Marine Science
California State University Monterey Bay, 2022

The widespread use and subsequent reuse of plastics in the agriculture industry increases the risk of improper disposal, posing a threat to important wetland habitats. When plastics degrade, they break up into smaller pieces that pose serious threats to organisms that ingest them and to habitats they settle in. This study quantifies the estimated concentration, types, and lengths of microplastics (< 5mm plastic particles) in the marsh environments of Elkhorn Slough, California's second largest estuary. Replicate samples of marsh soil samples were extracted from seven Elkhorn Slough marshes at varying distances from the head and the mouth of the estuary and potential sources of agricultural plastic. Using a safe and cost-effective density separation technique, microplastics were separated from the soil, identified, and counted on micro-filters using a dissecting microscope, then further analyzed with a Scanning Electron Microscope equipped with an Energy-Dispersive Spectrometer (SEM/EDS) to analyze surface microstructures and the elemental compositions of the particles. Two main microplastic morphotypes, fragments and fibers were observed. The average concentration of microplastics estimated by this study is ~1600 particles per kg of wet soil. Fragments are shorter but more abundant (making up 85% of microplastics found) than fibers and have an average length of ~85 µm and ~500 µm respectively. All microplastics found in collected samples exhibit signs of weathering, including pitting and fractures on the surface. I studied the particle size distributions of microplastics and fine-grained estuarian soil to highlight the similarities in the physical and hydrological influences controlling their distributions. This study helps to make conclusions about potential sources of microplastics to Elkhorn Slough and the Monterey Bay National Marine Sanctuary with an emphasis on California's agriculture industry and watershed dynamics. The microplastic particle size distributions reflect hydrological influences on the suspension and deposition of microplastics in the Elkhorn Slough watershed. This finding assisted in identifying plastic sources as non-local agriculture plastics immigrating from outside of this watershed due to the removal of a natural barrier and the unique hydrological dynamics of Elkhorn Slough.

TABLE OF CONTENTS

LIST OF TABLES

PAGE

LIST OF FIGURES

CHAPTER 1

INTRODUCTION

Early manufacturers of plastics underestimated the pervasiveness of the material in every industry and habitat on Earth because of their limited understanding of how to properly recycle and/or dispose it and their greater desire to sell it (Sullivan, 2022). Marine ecosystems worldwide are now teeming with high concentrations of microplastics (defined as plastic particles smaller than 5 mm) (Law, 2017). Primary microplastics, such as abrasive materials and virgin pellets, are manufactured at the "micro" size while secondary microplastics are fragments derived from larger pieces of plastic due to the breakdown and weathering of their simple polymer structure (Auta, et al., 2017). Early research on microplastics established typical morphological characteristics that can be used for categorization, which is useful for comparing current research quantifying microplastics across ecosystems. Microplastics can be categorized into morphological classifications based on the most found items: fragments, pellets, fibers/lines, films, foams, granules (Free, et al., 2014; Hidalgo-Ruz and Thiel, 2012). Microscopic erosional/dissolution patterns, or a lack thereof, are important indicators of the transportation history and residence time of the plastic particle in the environment.

While microplastic concentration is positively correlated with human population density (Thompson, et al., 2010; Scheurer & Bigalke, 2018), these persistent particles have also been found in the most remote parts of our world from the deep sea (Van Cauwenberghe, et al., 2013) to the French Pyrenees (Allen, et al., 2019), and in environmentally protected areas including National Marine Sanctuaries (Choy, et al., 2019) and National Parks worldwide (Free, et al., 2014; Whitmire, et al., 2017). Over the last decade, research on microplastics in the marine environment has increased dramatically because early studies found large amounts of small debris in the middle of ocean gyres, leading scientists to discover that oceans are sinks for much anthropogenic plastic debris (Browne, et al., 2011; Law, 2017; Andrady, 2011; Moore, 2008; Thompson, et al., 2004).

To understand where these small plastic debris that are found in the middle of our oceans come from, we must examine our rivers and freshwater sources. A model estimate for the plastic input from rivers to our oceans ranges from 1.15 and 2.41 million tons per year, but there is still the need for extensive monitoring of plastic contamination on freshwater ecosystems that exchange water with the ocean (Lebreton, et al., 2017). Unfortunately, finding and studying microplastics in these dynamic habitats is challenging because of the high amount of organic matter in the sediment and water column and because sediment particles share physical characteristics with microplastics, making them difficult to identify. This study tackles this issue by exploring the distribution of microplastics in the Elkhorn Slough estuary, which experiences a tidal exchange with the Monterey Bay National Marine Sanctuary, where a 2018 study found microplastics composed of polyvinyl chloride (PVC) and polypropylene (PP) throughout the water column (Choy, et al., 2019).

Research on microplastics is a developing field, particularly in terrestrial and freshwater ecosystems. Previously published works on microplastics in estuarian habitats have observed a range in microplastic concentration and type (Table 1). Microplastic research in estuarian habitats is generally lacking and results are difficult to compare across studies due to a lack in standardization (Table 1). The source of microplastics in estuaries is important to consider because estuaries are vital ecosystems that bridge terrestrial and freshwater to marine habitats. This study focuses on Elkhorn Slough, a wetland in the heart of California's agriculture fields, where acres of plastic are sprawled over hills and valleys to the Pacific Ocean.

Table 1 Studies on microplastics and their reported concentrations in estuarian habitats

Location	Habitat Type	Microplastic Concentration	Most abundant type of MP found	Reference
Changjiang Estuary, China	Estuary	20-340 (Items/kg dry sediment)	Fibers	Peng, 2017
Tamar Estuary, UK	Estuary	<1-8 (Items <1 mm/ 50 mL sediment)	Fibers	Thompson, et al., 2010
St. John's Lake, UK	Estuary	2.4 (fibers/ 50 mL sediment)	Fibers	Thompson, et al., 2004
San Francisco, USA	Estuary	0.1-11 (Items/ g dry sediment)	Fibers	Sutton, et al., 2019

Note: the reported units for microplastic abundance are not consistent because a standard unit system has not yet been established

Estuaries are important study sites for microplastic research because they connect ecosystems and can be made up of many depositional environments like mudflats and marshes. An estuary’s depositional regime is controlled by physical processes like waves and tides which structure the sediment distribution by suspension, transportation, then deposition of particles according to their size and density (Thompson, et al., 2010). We can measure the rates of sediment erosion and accumulation over time to better understand how depositional regimes change over time. Depositional environments in estuaries, like mudflats and marshes, containing brackish water with slow water flow and high concentrations of organic matter can be a sink for small particles like clay and microplastics. Although there is no evidence for microplastics found in sediment with a high proportion of clay, their depositional behavior is relatively similar: they settle slowly and are deposited in areas where water flow is slower (Thompson, et al., 2010; Scheurer & Bigalke, 2018). This similarity is important because it can reveal where microplastics can settle.

Investigating estuaries as a potential sink for microplastics can uncover gaps in the current knowledge of how and where microplastics are transported. While microplastics float on the sea surface, they are subject to biofouling by micro- and macro-organisms, which increases microplastic density, causing them to be negatively buoyant, and sink to the seafloor (Fazey & Ryan, 2016; Chubarenko, et al., 2018). Biofouling can increase microplastic's density and cause rapid mechanical degradation on the surface of microplastics (Andrady, 2011; Fazey & Ryan, 2016). The physically dynamic habitats found in estuaries such as shallow intertidal marshes and mudflats are unique locations for chemical and mechanical degradation because they are influenced by tidal fluctuations in UV radiation, temperature, salinity, and dissolved oxygen (Weinstein, et al., 2016). Although estuaries can be a potential sink for microplastics, it also is likely an important degradation zone where they can easily be broken into smaller particles and distributed in wider spatial ranges.

PLASTICS IN THE AGRICULTURE INDUSTRY

In 2017, estimations of plastic use in the global agriculture industry reached 6.96 million metric tons that year alone (Jansen, et al., 2019). In 2016, the estimated annual input of microplastics by farmlands in North America ranged between 44-300 thousand metric tons (Nizzetto, et al., 2016). Table 2 is an incomplete list of typical plastic uses in the agriculture industry with their polymer type and colors developed by Cornell University (Levitan, 2016). This table shows that plastics are ubiquitous in the agriculture industry and are made up of mainly polyethylene (both high density polyethylene and low density polyethylene) which has a larger surface area than other polymer types, making it more susceptible to organic pollutants (Wang, et al., 2016). All of these plastic types will erode away in the fields, and many are not recyclable.

Disposing of these plastic products is difficult; many facilities cannot recycle certain types of plastic and plastic with any organic residue. Elkhorn Slough runs through Monterey County, where the Monterey Regional Waste Management District reported that 5,700 tons of plastic mulch film was landfilled in 2019 (Krone, 2020). An initial survey for this study of abandoned agriculture fields in Elkhorn Slough reported that the common types of plastic found were high-density polyethylene (HDPE) from black or blue drip tape, white PVC from piping, and black or clear polyethylene (PE) from plastic mulching. Without proper disposal methods for agriculture plastics, they are subject to mechanical and chemical degradation, leading to the introduction of secondary microplastics to terrestrial, freshwater, and marine ecosystems (Nizzetto, et al., 2016).

Table 2 Agricultural Plastic Products and their typical resin and colors. Adapted from Levitan, 2016

Agriculture Plastic Products	**Typical Resin**	**Typical Color(s)**
Bags for wood pellet, peat moss, soil amendments, etc.	PE	Wite, some with print &/or black interior
Bale netting	PE, PP	Translucent green, white, or blue
Bale wrap	LDPE, LLDPE	White, less commonly green or other colors
Drums (55 gallon container)	HDPE	various
Fumigation and solarization film	LDPE, LLDPE	clear or green
Greenhouse, hoophouse, tunnel covers, perforated row covers	LDPE, LLDPE	clear or white
Horticultural mulch film	LDPE, LLDPE	black, less commonly white, clear, or other
IBCs (Intermediate Bulk Containers)(a.k.a tote, pallet tank)	HDPE	Translucent/white
Irrigation pipe	HDPE	black
Irrigation drip tape	PE, PVC	black
Irrigation polytube	LDPE, LLDPE	white

Note: Plastic resin types are Polyethylene (PE), Polypropylene (PP), Low-density polyethylene (LDPE), Linear Low-Density polyethylene (LLDPE), High Density Polyethylene (HDPE), Polyvinyl chloride (PVC)

Microplastics enter the soil in agriculture fields from the plastic degradation processes mentioned above (Scheurer and Bigalke, 2018), sewage sludge and wastewater contaminated with microfibers (Browne, et al., 2011), organic fertilizers (Weithmann, et al., 2018), tire wear and tear (Kole, et al., 2017), and atmospheric deposition (Allen, et al., 2019). Agriculture fields worldwide, including those in Central California, use wastewater sludge for fertilizer. Despite regulations and extensive treatment processes, it is estimated that the mass of microplastics in the sludge applied to agriculture fields annually could exceed 400,000 metric tons (Nizzetto et al., 2016), which is more than the estimated mass of microplastics found on the surface of our world's oceans (estimated by Eriksen, et al., 2014 to be over 250,000 tons). Human civilizations have commonly grown crops along rivers and estuaries due to fertile soil but, in our modern civilization, we have introduced plastics to increase crop yield and protect harvests without researching the degradation of these plastics into these essential waterways that connect our human lives to the ocean. An example of this practice can be found in Monterey Bay, where highly concentrated agriculture fields surround protected wetlands.

STUDY SITE

ELKHORN SLOUGH, CA

Elkhorn Slough, located between Castroville and Moss Landing in Central California, is an 11.3 km long seasonal estuary that feeds into Monterey Bay. The average water depth in the slough and its tidal creeks is approximately 1.4 m with a tidal range of approximately 1.7 m in the main channel (McLaughlin, et al., 2006). In the 1940s, the dune barrier between Elkhorn Slough and Monterey Bay was opened, introducing the slough to more salt water and erosion from tidal currents (Broenkow and Breaker, 2005). At low tide, most of the slough is exposed and the main channel becomes narrow, whereas, at high tides, the surrounding mudflats are inundated with saltwater entering the slough. Flood tides carry in coastal waters from Monterey Bay at Moss Landing Harbor and reaches to Hudson Landing, close to the head of Elkhorn Slough (Broenkow and Breaker, 2005). Ebb tides remove about ¾ of the mean high-water volume daily, carrying with it sediment eroded from the banks and the bed of the slough directly into the Monterey Bay National Marine Sanctuary, and creating a plume extending 3 km or more offshore (Smith, 1973; Broenkow & Breaker, 2005). This exchange of water and sediment stretches across the Monterey Canyon to Moss Landing Harbor to California's Central Valley agriculture fields, likely transporting plastics of varying size ranges along the way every day.

Elkhorn Slough is an anthropogenically-modified estuary with a long history of surrounding agriculture use. This study will focus on local agriculture fields surrounding Elkhorn Slough as potential main source of microplastics to the watershed because agriculture fields make up 26% of land use in the Elkhorn Slough watershed (Caffery, et al., 2002). Before it was opened to Monterey Bay, Elkhorn Slough was diked and dammed to allow for extensive agriculture use around the slough and still is today (Broenkow and Breaker, 2005). Sand Hill Farms, located on the east side of Elkhorn Slough, was an active conventional farm for decades before it was abandoned in 2008. In 2016, the Elkhorn Slough Foundation purchased the property and began restoring the land, beginning with cleaning up the left-over plastics used for agricultural purposes. In 2002, the Elkhorn Slough Foundation purchased the 200-acre Chamisal Ranch property located by Carneros Creek that feeds into Elkhorn Slough. The Elkhorn Slough Foundation removed 180 metric tons of trash left over from the agriculture use on this property (Elkhorn Slough Foundation, n.d.). Presently, Rocha Brothers Farms LLC and Lazzerini Farms occupy several agriculture fields on the west side of Elkhorn Slough's main channel and the Elkhorn Slough Foundation owns and monitors agriculture land on the east side of the main channel (Figure 1C). These are just a select few of the active and abandoned agriculture fields that Elkhorn Slough is surrounded by where plastics are used and left to break down into microplastics.

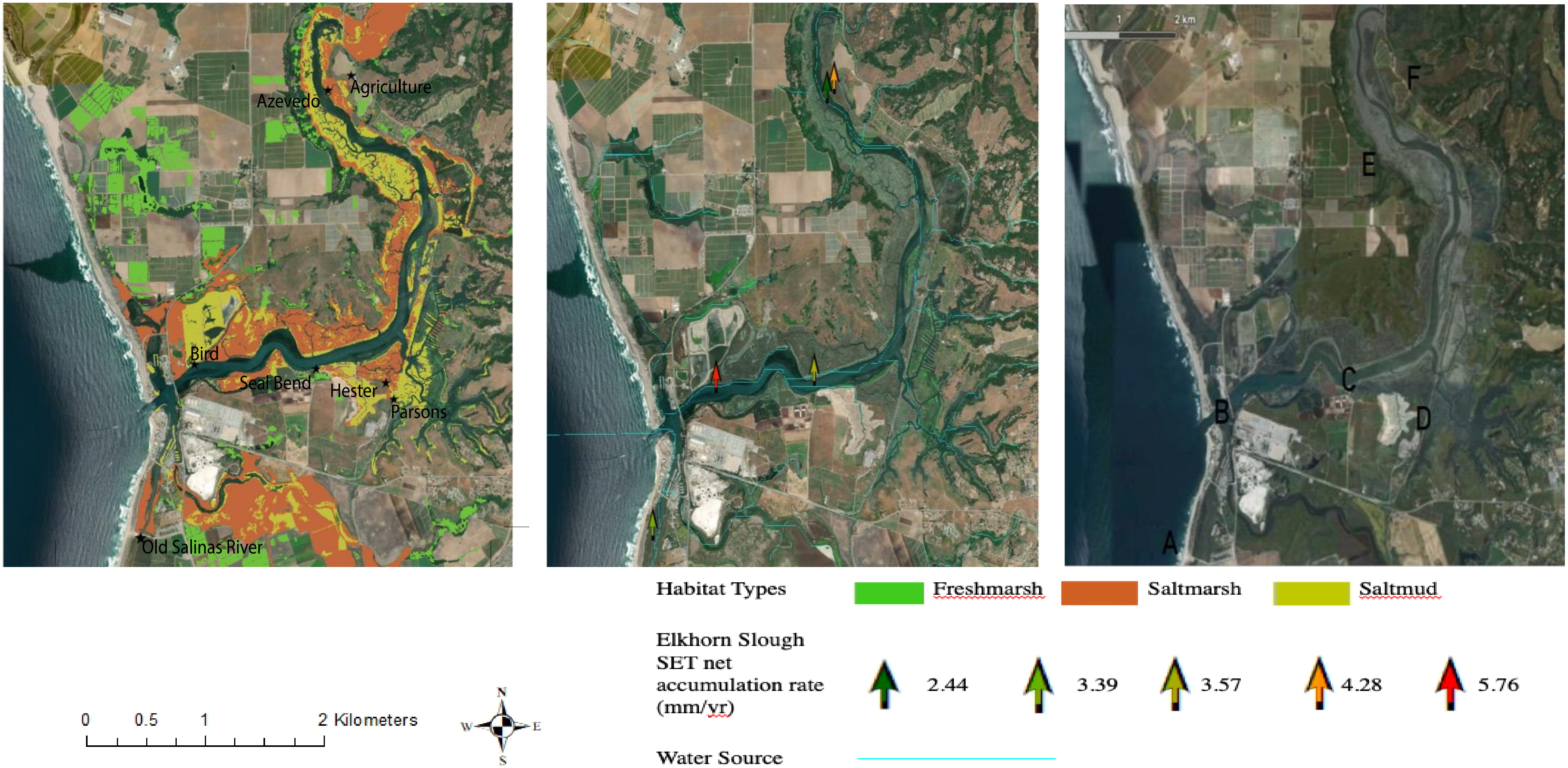

Figure 1 Maps of study location, Elkhorn Slough, located in Moss Landing, CA. Figure 1A Sample sites and their corresponding habitat types. Figure 1B Locations of Sediment Elevation Tables (SETs) and their corresponding net accumulation rates as indicated by color of arrows and water sources to Elkhorn Slough. Figure 1C Potential plastic sources to Elkhorn Slough: A) Old Salinas River B) Moss Landing Harbor C) Dairy D) Dump E) Agriculture Fields owned and operated by Lazzerini Farms and Rocha Brothers Farms LLC F) Elkhorn Slough Natural Preserve

Figure 1 shows a present-day Elkhorn Slough that is a result of numerous anthropogenic modifications transforming marshlands into irrigation systems, harbors, agriculture fields, and even a railroad. Beginning in 1866, a commercial wharf was built to support the booming agriculture, whaling, and fishing industries in the area as well as the increasing immigration due to California's Gold Rush (Moss Landing Harbor District, n.d.). Soon after, around 1890, the Pajaro Valley Consolidated Railroad was constructed on the wetlands of Elkhorn Slough (Moss Landing Harbor District, n.d.). In 1947, the Moss Landing Harbor was opened by dredging through the natural sand dunes for water way access and was eventually funded by PG&E's Moss Landing Power Plant, (Moss Landing Harbor District, n.d.). The numerous anthropogenic changes to important waterways in this region also influenced the water supply of acres of past and future farmland.

California supplies the United States with the majority of the produce the population consumes but has very few natural resources supplying freshwater to its agriculture fields. One of these important natural resources is the Salinas River, a 282 km long river used for irrigation in the most productive region in California beginning in the Garcia Mountains in San Luis Obispo County traveling northwestward through Salinas Valley and ending in the Monterey Bay National Marine Sanctuary (CoastView, 2019). The mouth of the Salinas River was diverted 6 miles south in 1906 due to an earthquake that devastated the region (CoastView, 2019). Now, there is an overflow channel called the Old Salinas River that runs from the new mouth to Moss Landing Harbor with dunes on the West side and agriculture fields on the East side. The Old Salinas River and Moss Landing Harbor are listed as Critical Coastal Areas by the California Coastal Commission which identifies potential sources of pollutants to be agriculture, urban runoff, miscellaneous, unpermitted discharges, natural sources, and unknown sources (California Coastal Commission's Water Quality Program, 2019). As of 2019, microplastics were not listed as a pollutant monitored by the California Coastal Commission, whereas PCBs, pesticides, and harmful bacteria (which can be transported by microplastics) are measured (California Coastal Commission's Water Quality Program, 2019).

Microplastics can pose serious threats to marine environments: diverse and numerous marine species unknowingly ingest microplastics, which can carry invasive species, and can adsorb persistent organic pollutants (POPs) (Moore, 2008). Many species that populate and migrate to Elkhorn Slough are historically found to be adversely affected by microplastic ingestion although there are no published studies on wildlife ingesting microplastics specific to Elkhorn Slough yet. Migratory shorebirds feeding and roosting in Elkhorn Slough's mudflats and salt mud could ingest plastics that could release contaminants into their tissues (Van Cauwenberghe & Janssen, 2014). These birds and marine mammals, like sea otters and harbor seals, feed on invertebrate species living in mudflats that have been found to contain microplastics translocating from their gut to their circulatory system (Thompson, Browne, & Galloway, 2010). Elkhorn Slough's surrounding agriculture fields populated by worms could potentially be in danger of ingesting microplastics which can transfer pollutants and additive chemicals into their gut tissues (Browne, et al., 2013). As they break down, Microplastics can introduce serious health hazards to the soil's microbiome because their large specific surface area allows them to adsorb toxic organic chemicals like perfluorochemicals (PFOS) (Yuan, et al., 2014), heavy metals (Brennecke, et al., 2016), and antibiotics (Li et al., 2018). Plasticizing agents, like phthalic acid esters (PAE), are loosely incorporated in the polymer structure of the plastic mulch widely used in agriculture fields in this region and can leach into the surrounding environment (Steinmetz, et al., 2016). These can cause health problems to organisms in a wide range of sizes and to the encompassing watersheds.

As previously stated, the tidal influence of Elkhorn Slough spreads 3 km offshore into the Monterey Bay. Under the sea surface lies the 4 km deep Monterey Canyon populated by scarce but opportunistic feeders (Choy, et al., 2019). A 2019 study in the Monterey Bay found Polyethylene terephthalate (PET), Polyamide (PA), polycarbonate (PC) and polyvinylchloride (PVC) in the stomachs of pelagic red crabs and giant larvacean sinkers in the water column (100-150 m and 200-250 m water depth respectively) offshore of the Moss Landing Harbor (Choy, et al., 2019). This study can serve as an example of what organisms find microplastics readily available to them offshore of Elkhorn Slough within the tidal exchange range of this study.

STUDY RATIONALE

SAMPLE SITE SELECTION

This research aims to quantify microplastic concentration and their morphological trends in marshes by collecting soil samples around Elkhorn Slough. Sample sites were selected in marshes based on the following criteria:

1) Soil exhibiting active deposition
2) Exposure to different hydrologic conditions
3) Proximity to anthropogenic plastic sources

These criteria created a basis for the kind of background data I needed to collect before selecting representative sampling sites. Background data such as soil deposition rates provided by the Elkhorn Slough National Estuarine Research Reserve as SETs (Endris, 2020). details of the sampling locations (coordinates, number of replicates, and habitat type) and physical properties (total mass of soil collected and their average grain sizes) are shown in Table 3. By selecting sample sites from the upper, mid, and lower parts of the slough that encompass depositional environments, this study quantifies the abundance of microplastics with time and avoids collecting samples from soil layers that pre-date the use of plastics in the agriculture industry. The latter would introduce a bias in the microplastic concentration estimates.

Table 3 Sample sites and their physical properties

Sample Site	Coordinates	No. of replicates	Habitat type	Accumulation rate from nearest SET (mm/yr)	Distance from nearest SET (m)	Total Mass of soil (g)	Avg grain size of soil sample (µm)
Agriculture Main Sample	36.850407 -121.75372	4	Fresh marsh/ field soil	4.28	669	203	5.7093
Agriculture Sub samples	36.85031 -121.75388						
Azevedo	36.849352 -121.75654	4	Saltmarsh	4.28	25	174	5.7093
Parsons	36.807997 -121.74704	4	Salt Mud	3.57	2,450	197	8.363
Hester	36.810209 -121.74845	4	Saltmarsh	3.57	1,025	203	10.4727
Seal Bend	36.812147 -121.76036	2	Saltmarsh	3.57	1,314	101	3.1092
Bird	36.812904 -121.78114	4	Salt Mud	5.76	656	207	5.0289
Old Salinas River	36.790359 -121.79054	4	Freshmarsh	3.39	714	203	2.8962

Elkhorn Slough is a dynamic estuary exhibiting a range in salinity and productivity levels from the mouth to the head of the main channel. Sampling sites were selected in locations that would encompass the entire tidal range of Elkhorn Slough and in varying proximity to fresh and saltwater sources. The Monterey Bay supplies saltwater while the Old Salinas River supplies brackish water to Elkhorn Slough via the Moss Landing Harbor. At the head of Elkhorn Slough, Carneros Creek feeds freshwater into the main channel of the slough and runoff from agriculture fields and smaller slough channels flow into Elkhorn Slough throughout the watershed (Figure 1B). Precipitation rates also influence the salinity and productivity levels in Elkhorn Slough's water chemistry so it should be noted that this study was conducted before the heavy rainfall season (Caffery, Harrington, & Ward, 2002).

To account for all local potential plastic sources, this study sampled in marshes along the main channel of Elkhorn Slough in and adjacent to agriculture fields, a harbor, and a dump (Figure 1C). For this study, samples were collected from an active agriculture field (Agriculture) and from three locations (Azevedo, Old Salinas River, and Seal Bend) directly adjacent to active and abandoned agriculture fields (Table 4). Importantly, this study uses the Agriculture site and the Old Salinas River site as references to local agriculture sources due to their close proximity of active agriculture fields. The Bird site is located adjacent to the Moss Landing Harbor, a recreational and commercial fishing harbor to over 600 slips used year-round. The Hester and Parsons sites are located between the main channel of Elkhorn Slough and a dump yard for cars and scrap metal next to Hester marsh. Considering previous studies have linked car tires to microplastic pollution, this site could be considered a potential source of microplastic to Elkhorn Slough (Kole, et al., 2017).

Table 4 Anthropogenic activities in the region studied and their distances from sample sites

Sample Site	Anthropogenic Activity	Approximate distance between Sample Site and Anthropogenic Activity(m)
Agriculture	Agriculture field	6
Azevedo	Agriculture field	356
	Railroad	28
Parsons	Railroad	7
	Dump	537
Hester	Railroad	825
	Dump	1031
Seal Bend	Dairy	184
	Agriculture field (abandoned)	4
Bird	Moss Landing Harbor	474
	Boat House	977
Old Salinas River	Agriculture field	12

Note: Distances are presented as hydrological distances

To study the distribution and calculate an estimated concentration of microplastics in Elkhorn Slough, replicate soil samples were collected from seven locations in the wetlands encompassing the area in and around Elkhorn Slough using glass jars and metal spoons. All the soil collected was sieved over 5 mm sieve to capture all contents that are less than 5 mm. Then, 50 g of soil was combined with 200 mL of 3% H_2O_2 to digest organic matter. After digestion, 200 mL of NaCl solution with a density of 1.2 g/cm^3 was mixed in with the soil to allow for the more dense soil to settle and the less dense microplastics to float. The solute with the floating microplastics was transferred to a filter via glass pipette and vacuum filtered. The filters were examined with a microscope for microplastics and the morphological type (fiber or fragment), size, and count of microplastics present on each filter was recorded. Further analysis on the microplastic's surface microstructure was examined with SEM by transferring the microplastics to a stub with carbon adhesive. The elemental makeup of the microplastics was analyzed using the attached EDS. Statistical analysis on the microplastics' length and location was used to understand trends in microplastic transportation in a wetland environment. See Appendix D for a flowchart outlining the sample processing steps.

STUDY OBJECTIVES

The main goal of this study was to establish, for the first time, a baseline of the concentration, type, and size distribution of microplastics in marsh soils in Elkhorn Slough and understand their potential sources. This overarching goal was achieved with these three main objectives:

1. Test a previously published method for extracting microplastics in sediments (e.g. beach sand) for estuarian mud
2. Estimate the concentration of microplastics in the marshlands of Elkhorn Slough
3. Assess the relationship of microplastic type, size, and concentration to physical dynamics and anthropogenic influences in Elkhorn Slough

Collecting data to support the objectives of this study was carried out using a select few laboratory instruments. These are outlined in Table 5 with the corresponding study objectives.

Table 5 Study objectives and their corresponding instruments

Study Objective	Instrument	Data Collected
Grain size of soil	Beckman Coulter LS 13 320 Laser Diffraction Particle Size Analyzer	Grain size (µm)
Length and type of MP	Leica S8AP0 & Leica EC3 Camera	Length of MP (mm) and type (fragment or fiber)
Microsurface structures of MPs	SEM Hitachi S-3400N	Evidence of weathering
Elemental analysis	EDS INCA software	Elements in MPs

CHAPTER 2
METHODS

SAMPLING IN ELKHORN SLOUGH

At each marsh site, Bird, Seal Bend, Hester, Parsons, and Azevedo, replicates of wet soil samples were taken using glass jars in four adjacent locations approximately 5 to 10 meters apart. At the Agriculture reference site, replicate samples were collected differently: one replicate was taken directly from the agricultural field while three replicates from soil running off from the agriculture field to the marsh plain of the Azevedo site. At the Old Salinas River site replicates were collected in the intertidal marsh directly adjacent to (approximately 10 meters away from) an active agriculture field. Sampling was carried out using 600 mL glass jars and metal spoons to avoid plastic contamination. The top 5 cm of mud was scraped off and sample jars 28 cm in length were pushed into the ground, collecting approximately 100 to 200 g of wet soil. The jars were immediately sealed with metal and sieved over a 5 mm metal sieve at the laboratory. Plastic pieces larger than 5 mm were saved for microscopy.

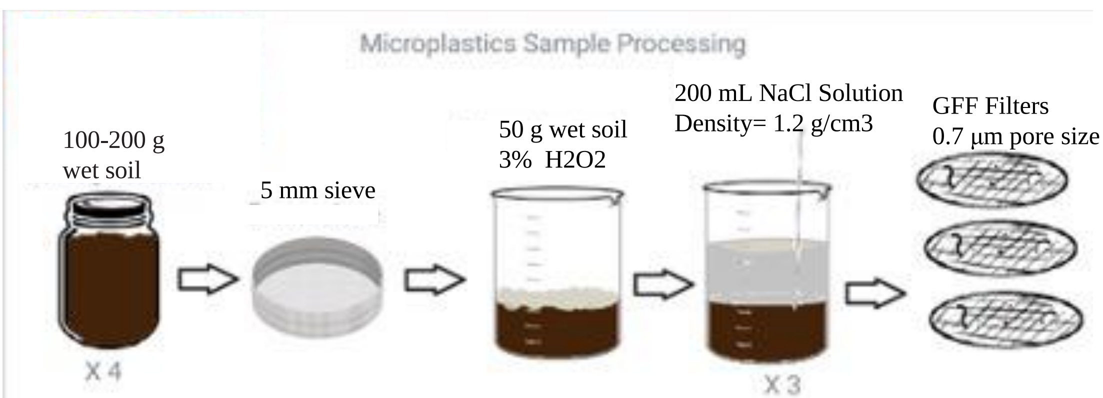

Figure 2. Sample processing steps used in this study.

SAMPLE PROCESSING

For this study, soil samples were not dried due to the small grain sizes forming hard conglomerates that are difficult to break and could risk damaging microplastics (Vermeiren, et al., 2020). From the bulk samples, 50 g of soil were separated and soaked in 200 mL of 3% H_2O_2, heated on a hot plate, and stirred intermittently until organic matter was not visible, and bubbles stopped forming for approximately 3 to 5 days (Figure 2). This study utilized a relatively low concentration of hydrogen peroxide of 3% instead of the commonly used 30% to eliminate organic matter in the wet soil samples because it is less toxic, more accessible, inexpensive, and, thus, easier for replication (Free, et al., 2014; Claessens, et al., 2013). To prepare for the density separation step, I removed excess H_2O_2 because it can cause the density of the solute to be lower than the desired density of 1.2 g/cm^3. The excess H_2O_2 was pipetted, filtered, and inspected for microplastics, which were not included in the final data for this study.

To separate plastics from the wet soil, this study used a density separation technique first proposed by Thompson, et al., 2004 and later tested by Besley, et al., 2017 wherein a NaCl solution with a density of 1.2 g/cm^3 is mixed with the sampled sediment (Figure 2). This causes the less dense plastic particles to separate from the sediment and float to the top of the dense solution. Using a glass pipette, the solute containing the floating particles is extracted and transferred to GFF glass microfiber filters (pore size .7 µm) and vacuum filtered. On the same sample of 50 g of wet soil, this density separation was repeated three times for every replicate from each site.

This density separation technique has been widely used with different solutions and sediment types. To test if this density separation technique captures a majority (> 50%) of microplastics, the process explained above was preformed 10 times on four samples from sample sites representing the tidal range of Elkhorn Slough. Performing more density separations on more samples was beyond the scope of this study.

Avoiding Contamination

To avoid contamination of the samples during processing and analysis from microplastics entering from clothing, materials used, and the atmosphere, this study followed strict guidelines. While collecting samples in the field and during sample processing, brightly colored clothing made of 100% cotton was worn to be detected under the microscope if any fibers shed. Metal spoons and glass containers were used to collect and store samples in the field. Immediately after collecting samples, they were stored in a closed room with filtered air vents to minimize air contamination. During processing, blank filters were left out and analyzed under the microscope for microplastics. All metal instruments and class beakers and flasks were covered in aluminum foil. Filters were stored in aluminum folded sheets for easy storage.

IDENTIFYING MICROPLASTICS

The following criteria for identifying a microplastic proposed by Noren, 2007 and later adapted by Hidalgo-Ruz and Thiel, 2012 and by Mohamed Nor and Obbard, 2014.

1) No cellular or organic structures are visible.
2) Fibers should be equally thick throughout their entire length.
3) Particles must present clear and homogeneous colors.
4) Fibers are not segmented or appear as twisted flat ribbons.
5) Particles are not shiny.

A Leica S8AP0 dissecting microscope was used to analyze all filters following the extractions using mainly 8 *10 zoom. Using a Leica EC3 digital camera attachment and proprietary software, LAS EZ, particles that followed the criteria for microplastics stated above were photographed and categorized manually as a “fragment” or a “fiber”. A “fiber” microplastic is a plastic that is significantly longer in one dimension than wide in the other two dimensions (Hartmann, et al., 2019). For this study, all particles found that were not in the form of fibers were either in the form of a round pellet, an irregular shape, or a film and were classified as “fragment”. Using the LAS EZ software’s measuring tool, the length (in mm) from the particle’s furthest ends was calculated, sometimes from segments in the cases of long fibers like Figure 3. Please see Appendix A for full list of all microplastics found with their categorized morphology and length.

Figure 3. Red fiber from sample site Hester and measurement sections in mm.

SEM Analysis

To detect evidence of weathering on the microsurfaces of the microplastics found on the sample filters, this study compared the unused and used abandoned plastics cut to approximately 2 mm. Reference stubs were made using cuttings from macroplastics (plastics larger than 5 mm) found in the agriculture field abandoned as trash and from "pristine" macroplastics from retail manufacturers (Table 6). Fragment and fiber microplastics from sample sites were carefully transferred to SEM stubs and secured with a Carbon sticker. A select few microplastics from all sample sites were observed under the SEM and this study found no particles that falsely appeared to be microplastics based off the criteria stated above.

Table 6 Reference fragments and fibers used on SEM stubs

Reference fragments	Reference Fibers
woven sheeting	nylon
drip tape	PVC fiber
PVC pipe	polyester
green mulch film	cotton
black mulch film	
gardening pot	

Photos were taken of pristine macroplastics (referred to in Table 6) and compared to the microplastics found in all seven sample sites. The surface microtextures were compared visually for signs of weathering. Based on surface microfeatures, microplastic particles have been identified as unweathered, having incipient alteration, showing conchoidal or linear fractures, jagged edges, or being highly degraded (Chubarenko, et al., 2018; Hidalgo-Ruz and Thiel, 2012

The following methodology outlines the preparation and settings used to analyze microplastics with the SEM Hitachi S-3400N. This study analyzed six SEM Aluminum stubs with a 15 mm diameter uncoated (i.e. non covered with conductive material such as Au or C) and prepared with a Ti standard for microanalysis. Using the secondary electron detector, samples were analyzed at a beam energy of 5 kV and a probe current of 10 μA at a vertical distance of ~5 mm from the stub. While acquiring SEM images some of the plastic particles exhibited signs of charging because the specimen was not coated with a conductive material and most of the microplastics imaged were irregularly shaped, which can cause the beam electrons to bounce off the object and escape at different angles (Newbury, et al., 1986). Plastics are mostly made up of Carbon, which has an atomic weight of 12.1 amu, hence the high amount of photons produced. Previous microplastic studies using a SEM experienced this charging effect while operating under similar settings to this study due to their omission of a metal standard but this study minimized this possibility by attaching a metal standard on the stub (Gniadek & Dąbrowska, 2019).

Grain Size Analysis

To understand the relationship between microplastic particle size and sediment particle size, a Beckman Coulter Laser Particle Size Analyzer (LPS) LS 13 320 measures the grain sizes of subsamples of collected soil. Subsamples (~2-3 g) from each replicate from the seven sample sites were pre-treated with H_2O_2 and sieved through a 2 mm mesh prior to adding the soil to the well (Beckman Coulter, Inc., 2011). In the LPS, a Fourier Lens focuses an incident beam and transforms scattered light projecting from electrons in the soil particles into a function of location on the detector plane (Beckman Coulter, Inc., 2011). This scattering pattern on the detector plane represents the contributions from all the particles in the sample and is transformed into a set of individual numbers corresponding to each size classification, which is used to understand the range in particle sizes in the sample (Lindon, Holmes, & Tranter, 2000). For this study, the mean grain size of each sample was noted and the distribution of particles in their size range was compared to the microplastics' size range (See Appendix E).

CHAPTER 3

RESULTS

MICROPLASTIC CONCENTRATION CALCULATED FROM 3 EXTRACTIONS

The data that this study conducted statistics on uses the concentration of microplastics recovered after just three extractions averaged between 3 jars. Figure 4 displays the total concentrations of microplastics at each sampling site. The sampling sites are arranged on the x-axis from the most northern portion to the most southern portion of Elkhorn Slough from left to right. The standard deviations calculated for each sampling site shows a small variance and range in standard deviations in concentrations between sampling jars.

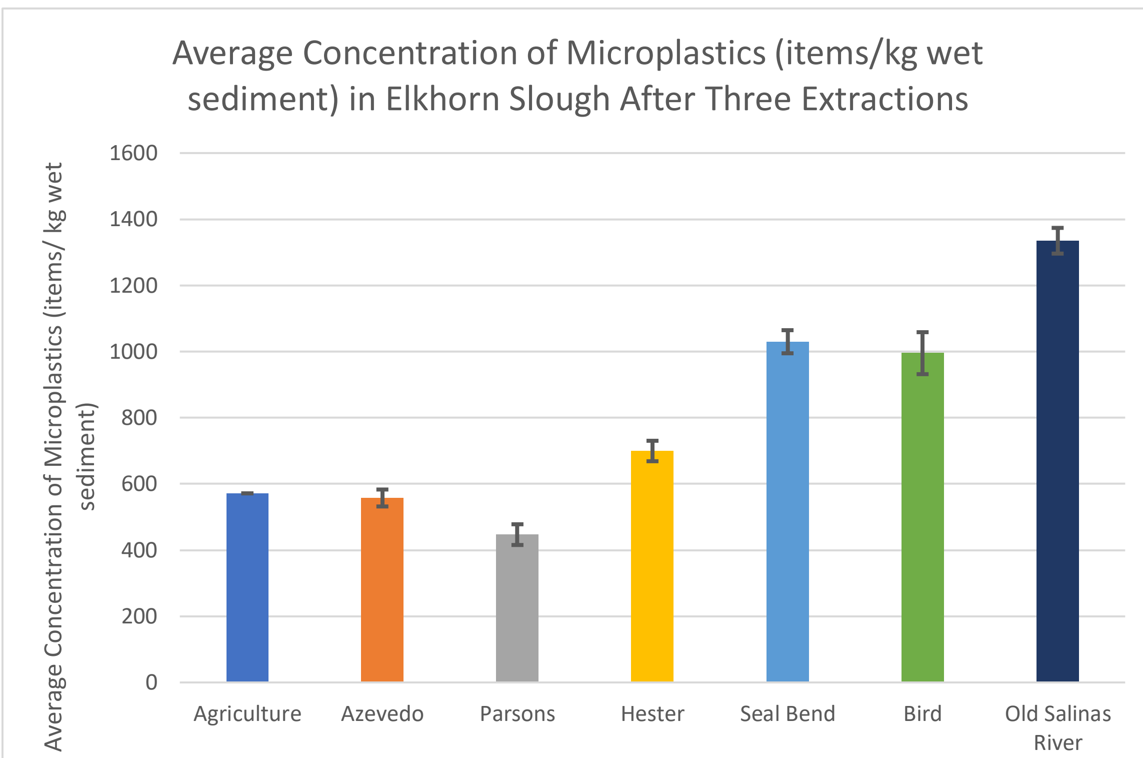

Figure 4. Concentration of microplastics (items/kg wet sediment) in the seven sample sites with standard deviation bars representing the standard deviation of concentrations within each sample site.

MICROPLASTIC MORPHOLOGY

While counting the microplastics manually, I identified and recorded the morphology of each microplastic using a dissecting microscope. The two morphological categories of microplastics used in this study were fragments and fibers. Table 7 shows the total abundance of microplastics classified as fragments and fibers and their respective proportions of the total. These reported numbers are counts from the original three extractions and should be considered underestimates.

Table 7 Total abundances of microplastics categorized as fragments and fibers

Site	# Fragments	# Fibers	total MPS	% Fragments	% Fibers
Agriculture	99	16	115	86.09	13.91
Azevedo	85	12	97	87.63	12.37
Bird	188	18	206	91.26	8.74
Hester	125	17	142	88.03	11.97
Seal Bend	92	12	104	88.46	11.54
Old Salinas River	250	21	271	92.25	7.75
Parsons	77	12	89	86.52	13.48
Total	916	108	1024	89.45	10.55

MICROPLASTIC LENGTHS

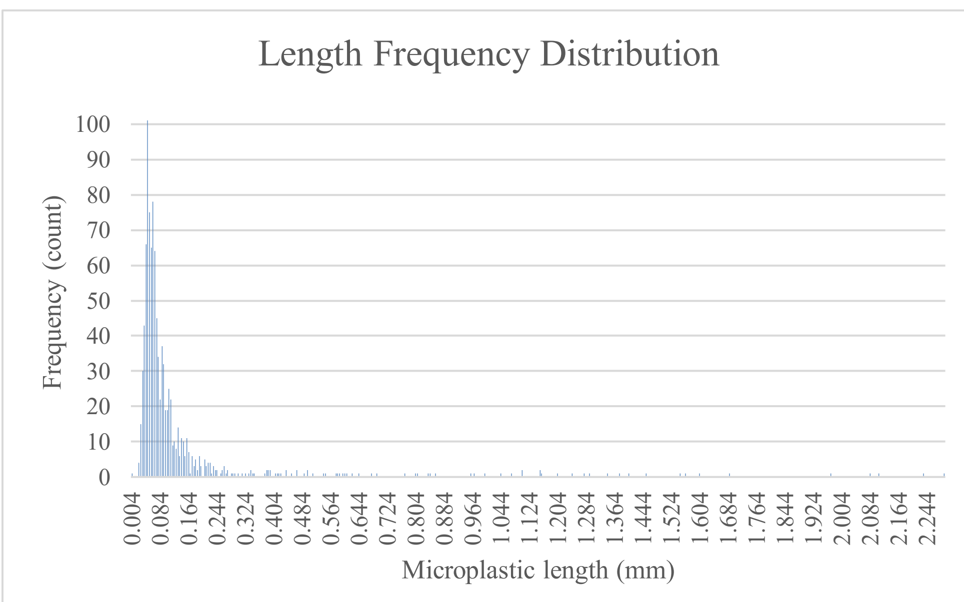

Figure 5 Length frequency distribution of all microplastics recovered after three extractions.

Figure 5 shows the frequency distribution of the relative abundance of microplastics lengths, separated in 35 bins, each representing 0.070 mm increments. As the plot shows, even though microplastic particle sizes range between 0.004 mm and 2.244 mm, the majority of the particles fall in the small size range, producing a right-skewed distribution. This results in a non-Gaussian distribution when the data are plotted in an arithmetic x-axis.

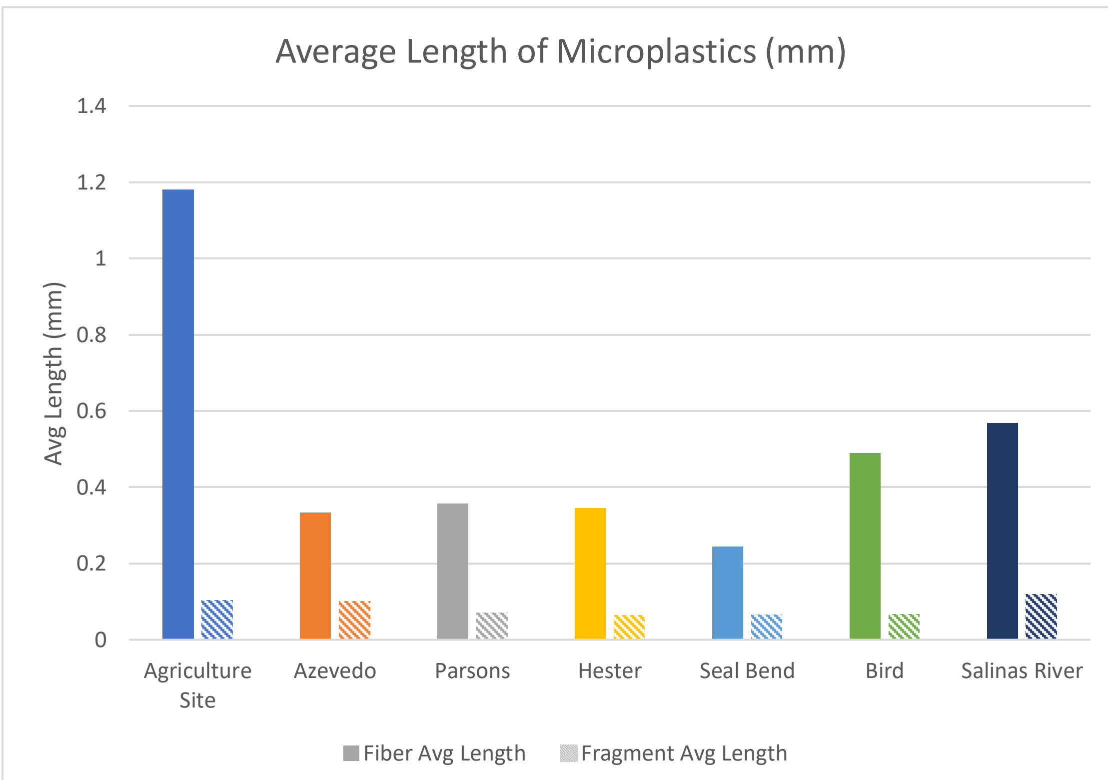

Figure 6 Average length (mm) of fibers and fragments found in Elkhorn Slough soil with fibers and fragments separately as indicated by solids (fibers) and stripes (fragments).

Figure 6 shows the average lengths of microplastics in all seven sites calculated by the finding the mean length of all microplastics found in the four replicate samples collected from each sample site. The average length was found by calculating the mean length of all fibers and the mean length of all fragments found in each of the replicates from all seven sample sites. Although mostly fragments were found in this study, it is apparent that the fibers found had a longer average length and there is little variability between the fragment lengths (Figure 6). The average lengths of the fibers and fragments are largest at both the agriculture reference sites (Agriculture Site and Old Salinas River). The smallest average lengths are observed in the fragments from sampling sites along the main channel of Elkhorn Slough.

MICROPLASTIC CONCENTRATIONS FOLLOWING MULTIPLE EXTRACTION TESTS

To test the percent yield of microplastics extracted from sediment using a technique proposed in the available literature for similar sediments (e.g. Thompson, et al., 2004), I performed 10 density separations on four samples from sites Agriculture, Azevedo, Hester, and Old Salinas River. The proportion of microplastics found after each density separation was calculated based off the total number of microplastics counted after 10 density separations. The results indicate that performing three density separations on the same sediment sample captures between 32.03% and 71.95% of microplastics, so the results of this study should be considered underestimates (Table 8). To capture 100% of microplastics, I would need to perform up to 10 density separations and subsequent extractions on all 26 replicates and analyze all 260 filters each for microplastics, which was beyond the scope of this study (Table 7).

Table 8 Microplastics quantified after 10 extractions

	Hester		Old Salinas River		Agriculture		Azevedo		
Extraction #	**# MPs found**	**% of total**	**# MPs found**	**% of total**	**# MPs found**	**% of total**	**# MPs found**	**% of total**	**Average % of total**
1	12	9.38	26	31.71	15	19.48	16	20.78	20.34
2	16	21.88	22	58.54	10	32.47	22	49.35	40.56
3	13	32.03	11	71.95	11	46.75	5	55.84	51.64
4	18	46.09	5	78.05	8	57.14	8	66.23	61.88
5	17	59.38	7	86.59	10	70.13	3	70.13	71.56
6	14	70.31	3	90.24	5	76.62	10	83.12	80.07
7	15	82.03	0	90.24	3	80.52	7	92.21	86.25
8	10	89.84	2	92.68	3	84.42	2	94.81	90.44
9	7	95.31	5	98.78	7	93.51	3	98.7	96.58
10	6	100	1	100	5	100	1	100	100
Total	128		82		77		77		

To recognize the trend resulting from 10 density separations, I will now present the results of the cumulative amount of microplastics found after 10 separations. Although, the number of extracted particles decreases after each density separation, fewer particles were extracted at the 10th separation (Table 8). To analyze this trend and create a predictive model, the assumption was made that the 10th separation corresponded to 100% of the particles being extracted (Table 8). The cumulative percent trend was then fit ($R^2 = 0.996$) with a parabola equation (Figure 7). Based on this model tests, the average cumulative percent of microplastics recovered after three density separations was ~50%. For this reason, the results for this study should be considered as an underestimate but can give us an idea of the scope of microplastics present in the sampled area.

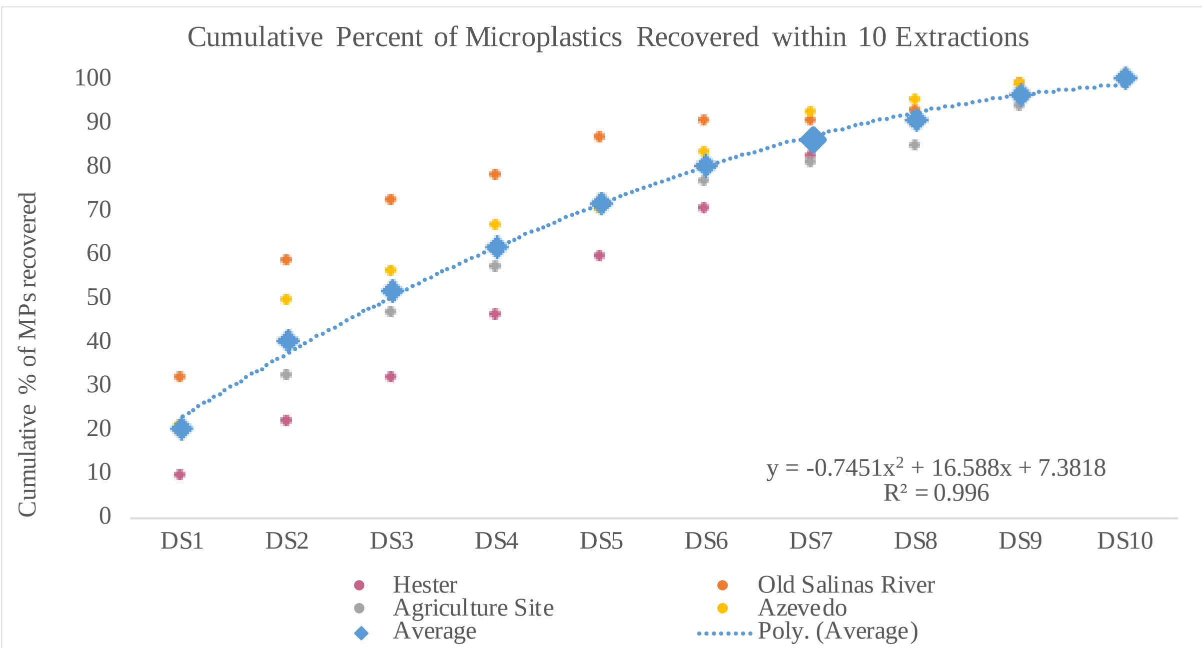

Figure 7. Cumulative Percent of Microplastics Recovered after each extraction following a density separation (DS). Polynomial function is fit based off the average cumulative percent of microplastics recovered from each extraction preformed on the four replicates tested.

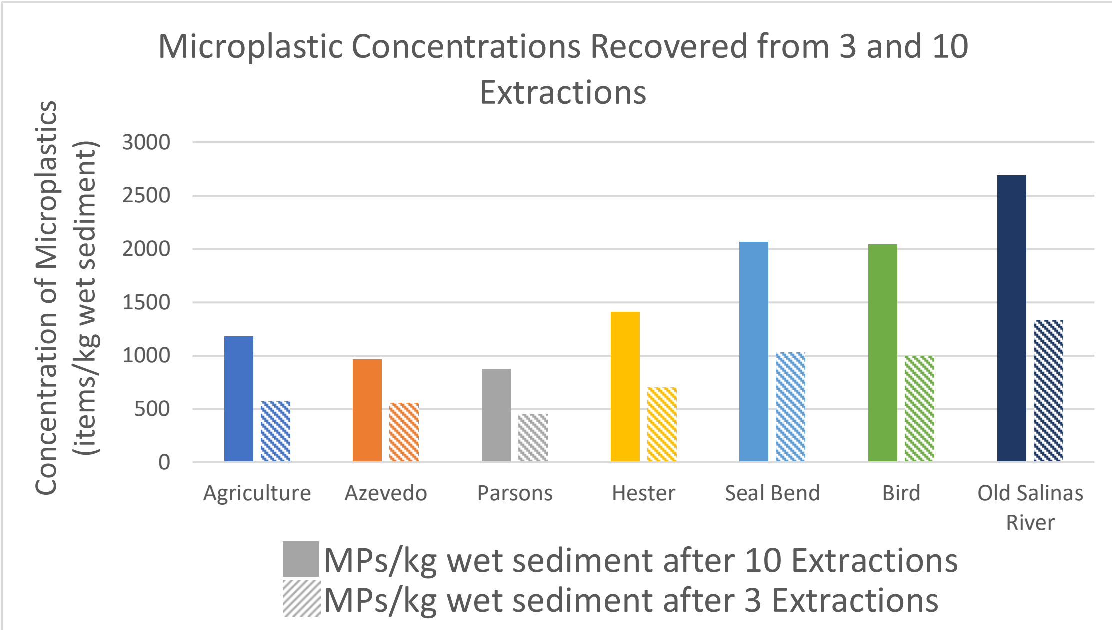

Figure 8. Concentration of microplastics (items/kg wet sediment) extrapolated after 10 extractions (solid bars) and after three extractions (striped bars). Microplastic concentrations after 10 extractions are extrapolated based off recoveries accounting for 50.4% of all microplastics.

Originally, 84 filters were analyzed for microplastic abundance across seven sample sites in and around Elkhorn Slough and are presented as striped bars in Figure 8. The concentration of microplastics extrapolated after 10 extractions (solid bars) shows the difference in microplastics that could have been recovered if I had performed up to 10 extractions on all replicates in each sample site. The estimated average concentration of microplastics using data collected from three extractions results in 806 particles kg $^{-1}$ whereas the estimated average concentration of microplastics recovered after 10 extractions results in 1602 particles kg $^{-1}$. Please see Appendix A for a full list of the microplastics found on each filter manually counted after three extractions.

CHAPTER 4

DISCUSSION

In total, 26 jars of mud were sampled across seven sample sites in marshes and agriculture fields in Elkhorn Slough, CA. In sum, 1024 pieces of plastic < 5 mm in length were extracted after three density separations and characterized by their morphology type and length. Both fragment and fiber types of microplastics were found throughout the estuary and were present in all jars.

Implications of the Concentrations of Microplastics Found in Elkhorn Slough

This discussion will begin by reviewing the abundances of microplastics found in Elkhorn Slough and an analysis on their sources and distribution using the data collected from three extractions. The sampling site with the highest abundance of microplastics after three extractions is The Old Salinas River site, with 271 microplastics, about three times as many microplastics as the Parsons sampling site (Table 7). The Old Salinas River meanders 282 km through California's central valley, passing hundreds of acres of agriculture land to Moss Landing, where the samples were collected (CoastView, 2019). Mostly fragments were found here rather than fibers (249 and 22 respectively) and had the largest mean length of fragments out of all the sampling sites. The high abundance of microplastics detected here could be caused by a larger supply of plastics to this river.

Besides the proximity to sources of plastics such as those stated in Table 4, the distribution of microplastics can depend on the environment's physical factors. The Bird sampling site is of importance because has the most microplastics out of the sites along the main channel of Elkhorn Slough, with 206 microplastics. This site is a popular shoreline fishing location and is in the closest in proximity to the Moss Landing Harbor where the slough and the Old Salinas River channel conjoin to meet the Pacific Ocean. The water from the Old Salinas River channel and the slough travels at the surface because it is less saline and dense than the offshore saltwater entering the slough from Moss Landing Harbor, which has a high salinity between 33-34 PSU (Smith, 1973). Flocculation of clay minerals can occur in estuaries where the difference in salinities and densities of the seawater and fluvial water can be detected, and ultimately results in an increase in settling velocities of the incorporated particles (Sutherland, et al., 2015). Incorporated particles can include microplastics; it has been found that aggregation between clay particles and microplastics increases with increasing salinity (Yang, et al., 2022). The proportion of clays in the sediment collected from Elkhorn Slough ranges from 13% to 64% and an influence of high salinity from seawater entering the slough provides an ideal setting for aggregation between clays and microplastics.

Previous studies have found no significant relationship between the proportion of fine-grained sediment in a sample and the abundance of microplastics but there is evidence to suggest that fine-grained sediment and microplastics can share settling behaviors (Thompson, et al., 2010; Chubarenko, et al., 2018). A recent study experimented with suspended organic and inorganic particles and introduced different concentrations of small PVC microplastics to understand the flocculation behavior in an estuarian environment (Andersen, et al., 2021). They found that the small PVC microplastics were likely to be incorporated in the aggregates and flocs that the suspended particles created and did not alter the settling velocity, indicating that flocculation can incorporate microplastics and settle them to the channel bed (Andersen, et al., 2021). The high abundance of microplastics found at the Bird site could provide evidence of microplastics incorporated in the flocculation of clay at this location in Elkhorn Slough.

Here, I will compare the results found after 10 extractions to other studies that have tested this method. Overall, after replicating the density separation 10 times, I found that the previously published density separation and subsequent extraction technique used for sediments and soils in other habitat types underestimates the percent of microplastics recovered when applied to estuarine soils and sediments. Previous studies have tested the density separation technique first proposed by Thomspon et el., 2004 for the yield of microplastics it can uncover. The density separation procedure used in this study was modified and tested by Besley, et al., 2017 on beach sediments. On average, that study recovered 93.3% of total microplastics found after four extractions, whereas this Elkhorn Slough study only recovered less than ~62% of the total microplastics, hence, the need to keep repeating extractions (Table 7 and Table 9). Another study found that this method underestimated their microplastics counts by spiking fine-grained sediment with microplastics and subjecting the sample to this density separation technique twice, resulting in microplastic recoveries ranging from 54.9% to 71.8% (Mohamed Nor and Obbard, 2014). The challenges associated with handling and processing fine-grained sediment is likely the cause of underestimating counts of microplastics and should be carried out with caution.

Table 9 Microplastics yields after 5 extractions adapted from Besley, et al., 2017

Microplastics counted from extraction filter papers, for 5 samples, with 5 repeat extractions. Including the percentage of total yielded from 1,2,3 and 4 extractions.

Extraction number	**Sample 1**	**Sample 2**	**Sample 3**	**Sample 4**	**Sample 5**	**Sample 6**	**Average**
1	14	12	9	4	5	3	7.8
2	7	8	5	9	3	14	7.7
3	17	3	3	3	4	4	5.7
4	1	5	2	1	4	1	2.3
5	5	3	1	0	1	2	2.0
Total	44	31	20	17	17	24	25.5
% from 1 extraction	31.8%	38.7%	45.0%	23.5%	29.4%	12.5%	30.2%
% from 2 extractions	47.7%	64.5%	70.0%	76.5%	47.1%	70.8%	62.8%
% from 3 extractions	86.4%	74.2%	85.0%	94.1%	70.6%	87.5%	83.0%
% from 4 extractions	88.6%	90.3%	95.0%	100%	94.1%	91.7%	93.3%

To put Elkhorn Slough's concentration of microplastics into context, I will compare it with microplastic concentrations presented in other studies that have sampled similar habitats characterized by fine-grained sediments such as those found in estuaries. Comparing abundances of microplastics to studies across different habitats and media should be done with caution because the methods for identification and extraction of microplastics differ with media type and no official unit of measurement exists yet. The average abundance of microplastics in Elkhorn Slough extrapolated from three counts based on the 10 extractions model is compared to the average abundances of microplastic particles kg $^{-1}$ in sediment from other locations around the world in similar habitats to Elkhorn Slough with similar sources of plastic (Figure 9). The average concentration of microplastics found in the sediment of marsh habitats in Elkhorn Slough is 1602 particles kg $^{-1}$ with small (0.04-0.07 mm) fragments accounting for the majority of microplastics found. After stating again that these comparisons should be taken with caution, the average concentration of microplastics in Elkhorn Slough seems comparable to larger bodies of water such as the Venice Lagoon (1423 particles kg $^{-1}$) and the harbors and channels of the Great Lakes, Gulf of Mexico, Long Island Sound, Atlantic Ocean, and the Mississippi River combined (1636 particles kg $^{-1}$). Compared to other estuaries, like the Changjiang Estuary (180 particles kg $^{-1}$) and the saltmarsh of Hangzhou Bay (264 particles kg $^{-1}$), Elkhorn Slough has considerably higher abundance of microplastics and more fragments than fibers. See Appendix F for a table comparing microplastic concentrations, morphology types, source types, and sampled habitats of the studies referenced in Figure 9.

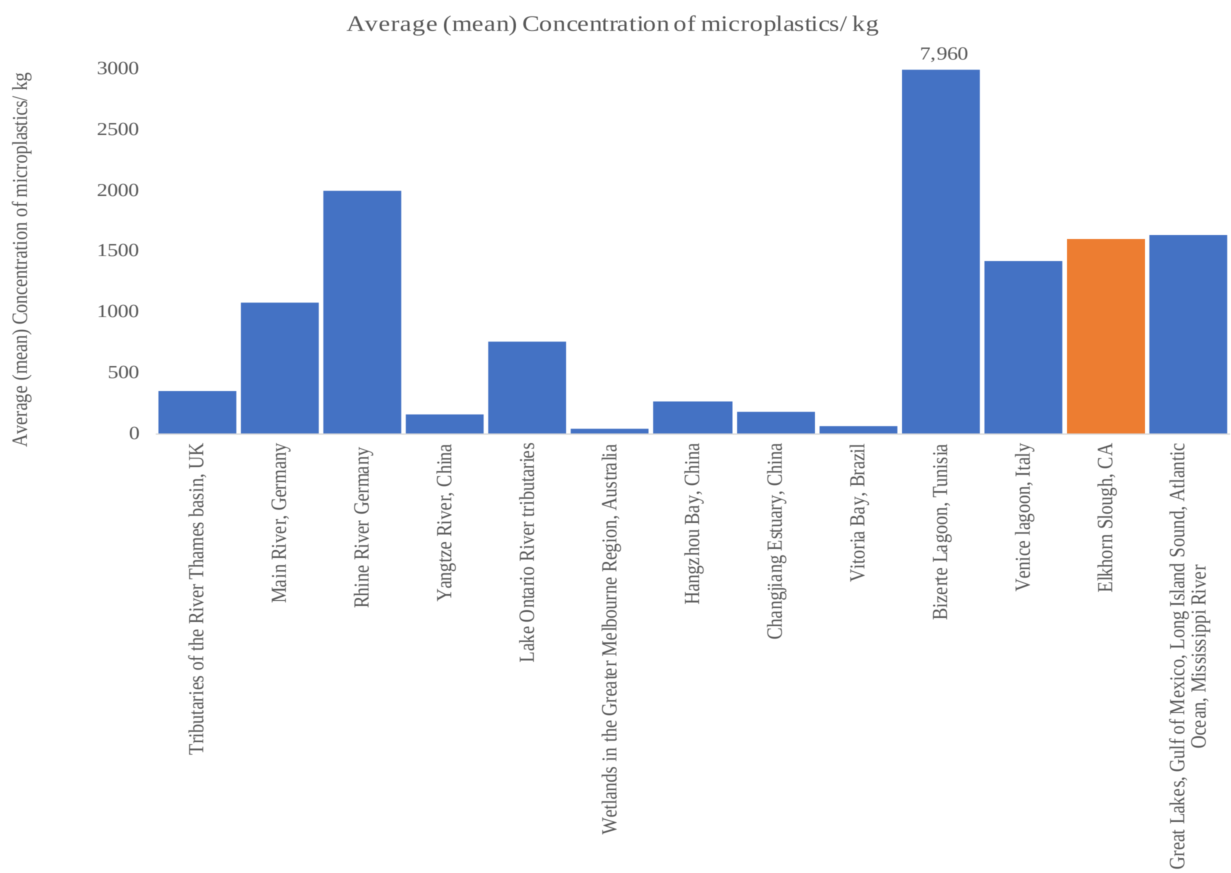

Figure 9. Average concentration of Microplastics (particles kg $^{-1}$ sediment) around the world in studies done on similar fine-grained sediments as Elkhorn Slough's (note: the methods used for the other studies are different from this study so the results of this comparison should be taken with caution)

Implications of microplastic size distributions found in Elkhorn Slough

The particle size distribution of the marsh soil at the microplastic sampling sites in Elkhorn Slough can be compared to the particle size distributions of the microplastics to visualize how they are distributed similarly in this estuarian environment. Since this study recovered mostly fragment types of microplastics (89% of total) and their settling behaviors are most like those of fine-grained sediment, which are also generally platy (e.g. clay minerals, micas), the length distributions of sediment and fragments are log-transformed and displayed in Figure 10 for comparison (Chubarenko, et al., 2018). Figure 10 reveals that the grain size distribution and the fragment microplastic particle size distributions display similar log normal distributions, but over different ranges of particle sizes. Specifically, the sediment particle sizes are smaller and the particle sizes of microplastic occur at the coarser tail end of the sediment grain size distribution. This suggests that the hydrological processes and residence times that control the size distribution of fine-grained sediment such as clay and silt also influence the size distribution of small microplastic fragments. Please see Appendix E for particle size statistics.

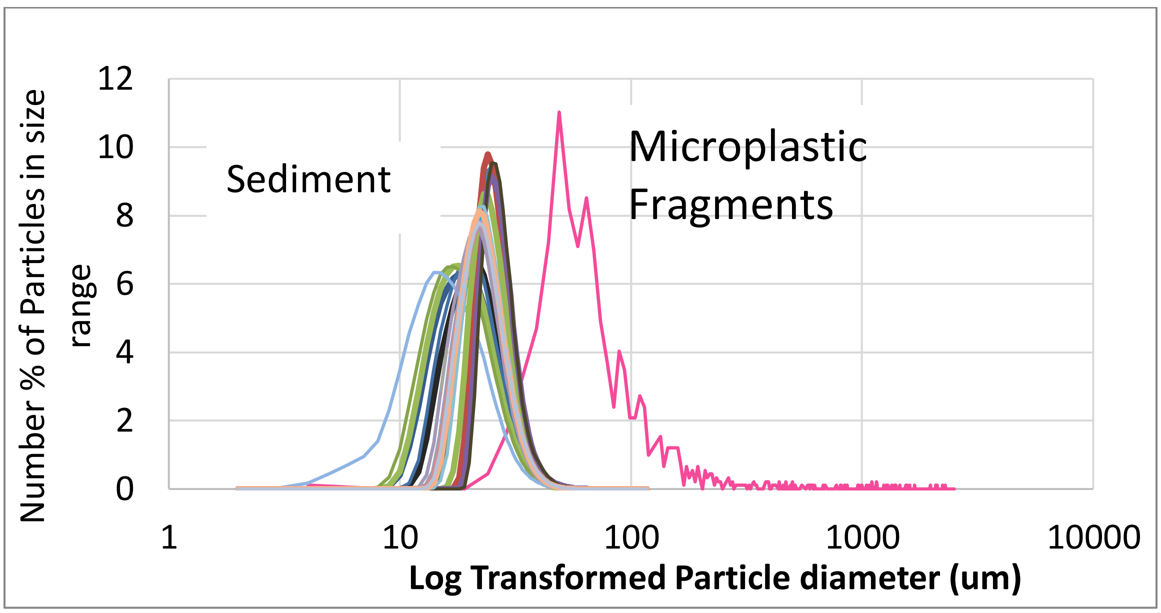

Figure 10 The percent of particles that fall within a specified size range for sediment grains and microplastic fragments in all sampling sites in Elkhorn Slough log transformed.

As shown in Figure 5, the distribution of the lengths of microplastics found in this study is skewed because of the higher abundance of small fragments. To perform the statistical calculations mentioned below, the lengths of all microplastics found are log transformed and determined as a log-normal distribution with a P-value < .05 using a lillie test function (Figure 11) (MATLAB, 2018). See Appendix A for statistics on microplastic lengths and Appendix C for the full results on the Student T Tests.

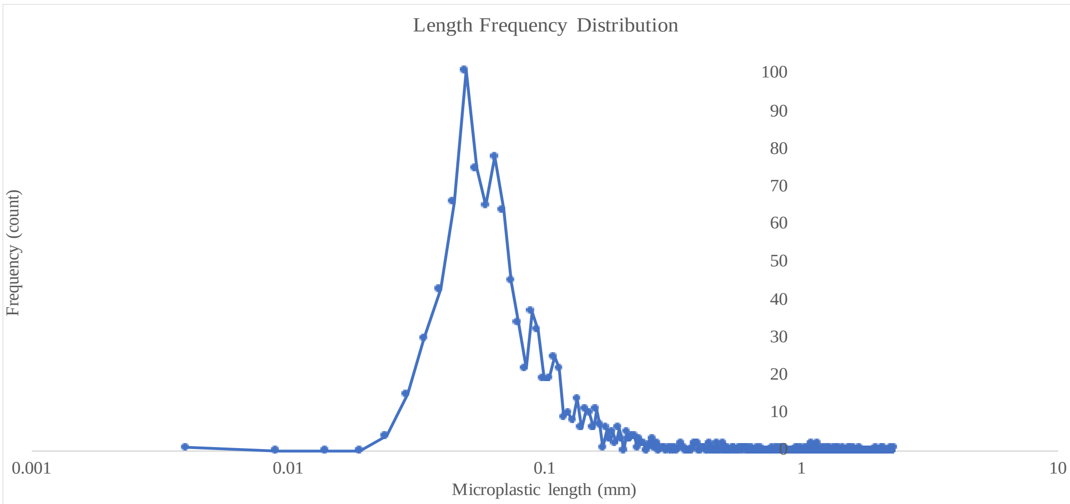

Figure 11 Frequency distribution (log transformed) of the length of microplastics (mm) found in Elkhorn Slough

To understand if there is any evidence of sorting and/or redistribution of microplastics due to their particle sizes, this study utilized Student T Tests between sampling sites. Student T Tests help to understand whether two sample means are taken from the same population. Here, I will present the P-values of the Student T tests calculated using MatLab comparing the log-transformed average lengths of microplastics to determine the association between sampling sites. In all Student T Tests, significance level was considered for P < .05 and the values highlighted in yellow are rejected.

Table 10 Student T Test Results for all MP lengths

	Agriculture	Azevedo	Parsons	Hester	Seal Bend	Bird	Old Salinas River
Agriculture		0.0169	0.0062	0.0002	0.0011	0.0001	0.0056
Azevedo	0.0169		0.4601	0.1752	0.1166	0.2716	0.3610
Parsons	0.0062	0.4601		0.5277	0.3659	0.8030	0.0915
Hester	0.0002	0.1752	0.5277		0.8647	0.6149	0.0073
Seal Bend	0.0011	0.1166	0.3659	0.8647		0.4953	0.0102
Bird	0.0001	0.2716	0.8030	0.6149	0.4953		0.0103
Old Salinas River	0.0056	0.3610	0.0915	0.0073	0.0102	0.0103	

Microplastic particle size distributions were originally hypothesized to display larger average lengths the closer the sample is to an agriculture field. To test this, I sampled at the two sites that are assumed to be directly affected by agriculture practices (Agriculture and Old Salinas River) and found that they are characterized by having larger average lengths in fragments and fibers combined compared to the rest of the sampling sites (Figure 8). The results in Table 10 indicate that the mean length was significantly different at the Agriculture Site compared to the other six sites, suggesting the frequency distribution of the microplastic particle sizes are different. The Old Salinas River site contains a microplastics population that is significantly different than the Bird, Hester, and Seal Bend sites as indicated by a P-value < 0.05. The low P-values do not give evidence to suggest that these local agriculture sites share similar size distributions amongst other sampling sites in Elkhorn Slough.

To understand the hydrological influences on particle transportation and deposition, the Student T Tests were used to compare the microplastic particle size distribution between sampling sites. Comparing the sample sites along the main channel of Elkhorn Slough, the P values of the Student T-test indicate that the difference in the sample means and SDs are not statistically significant; in other words, they come from the same population of microplastic length distributions. Overall, the Student T Test results provide support to the hypothesis that microplastics that deposit with the sediments on the marshes in various parts of Elkhorn Slough is homogenously distributed by hydrological processes across the estuary. In turn, the homogenous distribution of microplastic particle sizes, irrespective of the vicinity to potential local plastic sources (e.g agricultural fields) favors the interpretation that a significant portion of the microplastic is transported into the estuary from outside the local watershed. Most notably, these potential sources could be the Old Salinas River Channel and the Pacific Ocean.

SEM and EDS Findings

Here, I will conclude my discussion with observations on the microplastics' surface structures. Microplastic fragments extracted from the sediment samples were compared to cut fragments of plastic recovered from agriculture fields surrounding Elkhorn Slough and from unused plastics from the shelves of a hardware store. Using the SEM, plastic surface microstructures were observed for signs of weathering and erosion such as pitting, cracks, flaking, and adhering particles.

There are various types of plastic sheeting utilized for weed and insect barriers such as fumigation film, perforated row covers, and mulch film. This study focuses on a polypropylene woven landscape fabric, commonly used as mulch film. An unused cutting of a "Heavy-Duty PP Woven Weed Barrier" from Agfabric was compared to multiple microplastics found in Elkhorn Slough that shared similar structure to the fibers woven in the landscape fabric. This type of "woven sheeting" breaks down easily from its mesoplastic form by stripping off fibrous pieces until each microplastic fiber erodes away as shown in Figure 12B. The microplastics from the field exhibited adhering pieces possibly from biofouling or salt (Figure 12 C&D). The organic matter percent by weight (mg) in Elkhorn Slough ranges from about 0.7% to 13.4%, which suggests that biofouling could be occurring on the microplastics found. The low energy salt marsh and salt mud habitat in which these plastics were found could have supplied excessive amounts of salt for a prolonged time, causing the surface of plastics to crack. There also appears to be longitudinal grooves where the surface has been eroded away. This highly degraded surface looks comparable to that of polypropylene strips submerged in salt marsh habitat after removal of biofilm in Weinstein 2016.

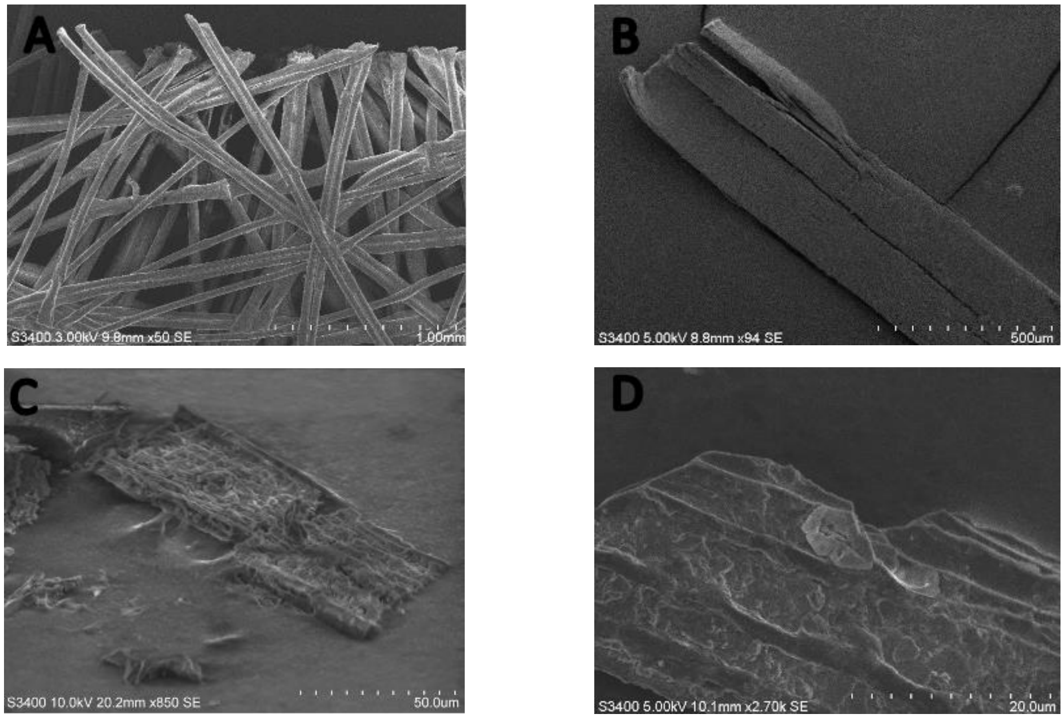

Figure 12 Woven sheet plastic in unused form from AgFabric (A), used form from an abandoned agriculture field in Elkhorn Slough (B), microplastic from Seal Bend sampling site (C), microplastic from Bird sampling site (D).

Plastic drip tape is widely used for irrigation and can be exposed to mechanical weathering from the soil, water, and sunlight. An unused cutting of drip tape compared to a cutting of drip tape recovered from an abandoned agriculture field reveals evidence of the various types of weathering this plastic encounters (Figure 13). On the rough surface of the microplastic found in the Agriculture Field sampling site, pitting is visible, and the texture appears to be more flakey, and there are cracks in the surface (Figure 13B). The microsurface texture of this sample has comparable evidence of weathering to that of microplastics submerged in salt water exposed to UV light in a controlled laboratory setting (Cai 2018).

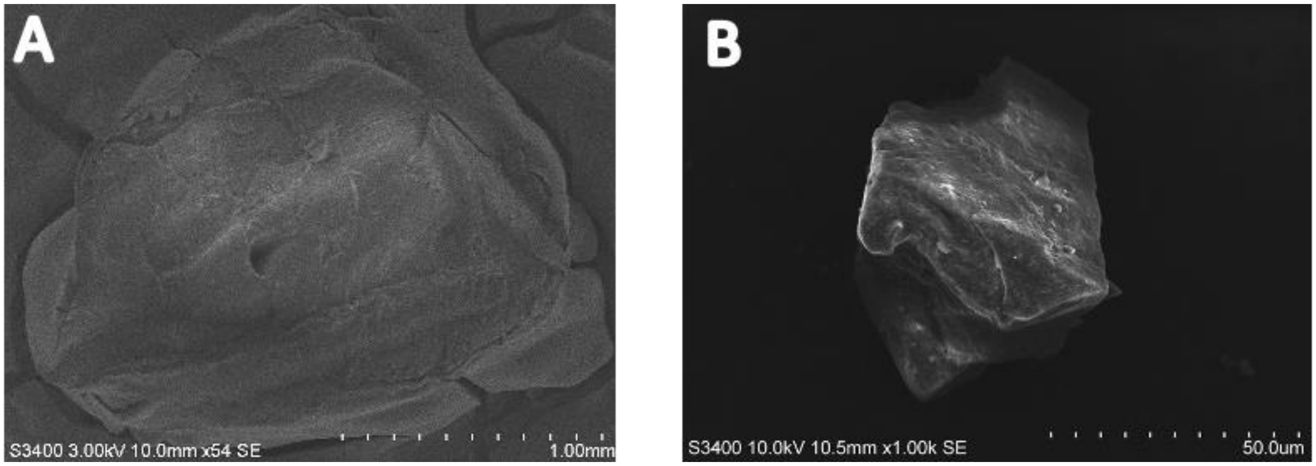

Figure 13 Drip Tape plastic from store shelf (A), and microplastic from the Agriculture sampling site (B)

Microplastics in the form of fibers extracted from the Elkhorn Slough samples were also observed for signs of weathering and compared to fibers from clothing. Fibers from the field appear frayed at the ends and exhibit signs of growth of either NaCl or organic matter on areas with more surface area. Fibers with a twisted helix design exhibited signs of erosion in the middle of the fiber, forming less weathered grooves on the sides of the fiber. Polyester and nylon fibers used as references showed no signs of fraying or erosion. Microplastic fibers are difficult to analyze using the SEM and the attached EDS due to their small diameter and density. This challenge and this study's findings of mostly microplastic fragments led to collecting EDS data on only the microplastic fragments from field samples.

This study utilized the EDS attachment on the SEM to understand if there was an association between the elemental composition of the microplastics found in the field and used and unused pieces of mesoplastics commonly used in agriculture practices. The difficulties associated with measuring the elemental composition of microplastics during this study were due to complications with the settings of the EDS and the low density, low atomic weight, and rugged surface structure of microplastics. Despite these complications, this study found that all samples analyzed contain Carbon and Oxygen. This study does not use Carbon and Oxygen as an indicator of plastic; many organisms and minerals contain these elements. The presence of Aluminum was apparent in most samples, but this could be due to the Aluminum stub used. Common background minerals such as NaCl and $AlSi_3$ were present in few samples and the elemental composition of the microplastic samples were corrected for these. This study found no trends or relationships between sample location and elemental composition.

CHAPTER 5

Conclusions and Future Research

This conclusion will begin with a recall to the study objectives and will detail how each goal concluded.

1. Test a previously published method for extracting microplastics in sediments (e.g. beach sand) for estuarian mud

2. Estimate the concentration of microplastics in the marshlands of Elkhorn Slough

3. Assess the relationship of microplastic type, size, and concentration to physical dynamics and anthropogenic influences in Elkhorn Slough

This study tested a safe and cost-effective method to separate microplastics from organic rich sediment using 3% H_2O_2, table salt (NaCl), and vacuum filtration for easy repeatability. Although this study found that preforming only three density separations per 50 g wet soil underestimates the abundance of microplastics, a parabolic function can be used to estimate the abundance of microplastics recovered after 10 density separations for four sample sites. The microplastic particle size distributions tested with Student T Tests reflect hydrological influences on microplastics in the Elkhorn Slough watershed. These findings identify plastic sources as non-local agriculture plastics immigrating from outside of this watershed then transporting and depositing throughout the Elkhorn Slough watershed.

The main purpose of this study was to measure the concentration of microplastics in the fine-grained sediment of Elkhorn Slough, an anthropogenically modified estuary in the heart of Central California's agriculture fields. The agriculture industry around the world heavily relies on plastic for cost-effective and efficient growing, transportation, and protection. This study estimates an average of over 1600 pieces of microplastics per kg of sediment in the marsh soils of Elkhorn Slough, the estuary that feeds directly into the Monterey Bay National Marine Sanctuary, a federally protected portion of the Pacific.

The SEM can help to understand how plastics break down in the natural environment. This study contributes to the very limited evidence we have of microplastics in marsh habitats. Future studies should focus on this apparent transition zone where microplastics travel in low-energy environments with fine-grained sediment, rich in organics, and slow-moving, shallow water exposed to sunlight and salt. Marshes and estuaries commonly connect to the ocean, creating a perfect pathway for anthropogenic debris to break down into microscopic pieces as they enter the ocean.

Research on microplastics in different locations must continue in order to uncover all of the sources of plastics to Elkhorn Slough. The San Francisco Estuary Institute has identified wastewater treatment plants and tires as main sources of fibers and fragments in their estuary soil. The agriculture fields in the watersheds of Elkhorn Slough and the Old Salinas River are permitted to use wastewater for irrigation. By collecting samples of the soil that uses wastewater irrigation, we can better understand where microfibers from our washing machines end up.

The Monterey Bay National Marine Sanctuary exchanges water with Elkhorn Slough through diurnal tides and could be transporting microplastics in the water column. Water column and channel bed sampling at the mouth of Elkhorn Slough could aid in the understanding of microplastic exchange and transportation in fluvial and seawater.

This research revealed that microplastics are found throughout the watershed and that the length distribution followed that of the fine-grained sediment it was sampled from, indicating that the hydrological conditions in Elkhorn Slough influence the distribution of microplastics throughout the whole watershed. The microplastics' length distribution and statistics results could indicate that their weathering occurs in agriculture fields and/or in other habitats (water column of the main channel, and/or mudflats) and is then distributed by hydrological processes. Unique hydrogeochemical processes like flocculation and biofouling are of importance to microplastic transportation and are present in Elkhorn Slough and estuaries worldwide. Flocculation fronts, where high rates of clay flocculation occurs, should be considered as study sites for microplastics because they could act as a sink for microplastics incorporated in the flocs and aggregates of fine-grained sediment.

Preliminary surveys did find mesoplastics in the reference agriculture field sites and most plastics found in these locations were microplastics. Because this study only collected samples from marsh habitats and one field, it is unknown what the microplastic concentration and corresponding length distributions are for other habitats in Elkhorn Slough.

REFERENCES

Allen, S., Allen, D., Phoenix, V. R., Le Roux, G., Durántez Jiménez, P., Simonneau, A., . . . Galop, D. (2019). Atmospheric transport and deposition of microplastics in a remote mountain catchment. *Nature Geoscience*, 339-344.

Andersen, T. J., Rominikan, S., Olsen, I. S., Skinnebach, K. H., & Fruergaard, M. (2021). Flocculation of PVC microplastic and fine-grained cohesive sediment at environmentally realistic concentrations. *Biological Bulletin*, 42-51.

Andrady, A. L. (2011). Microplastics in the marine environment. *Marine Pollution Bulletin*, 1596-1605.

Beckman Coulter, Inc. (2011, October 1). *beckmancoulter.com.* Retrieved from Instructions for Use LS 13 320 Laser Diffraction Particle Size Analyzer: https://www.beckmancoulter.com/wsrportal/techdocs?docname=B05577AB.pdf

Besley, A., Vijver, M. G., Behrens, P., & Bosker, T. (2017). A standardized method for sampling and extraction methods for quantifying microplastics in beach sand. *Marine Pollution Bulletin*, 77-83.

Broenkow, W. W., & Breaker, L. C. (2005). A 30-Year history of tide and current measurements in Elkhorn Slough, California. *Moss Landing Marine Laboratories Tchnical Report*, 55 p.

Browne, M. A., Crump, P., Niven, S. J., Teuten, E., Tonkin, A., Galloway, T., & Thompson, R. (2011). Accumulation of microplastic on shorelines woldwide: Sources and sinks. *Environmental Science and Technology*, 9175-9179.

Caffery, J. M., Harrington, N., & Ward, B. (2002). Biogeochemical processes in a small Californiaestuary. 1. Benthic fluxes and pore water constituentsreflect high nutrient freshwater inputs. *Marine Ecology Progress Series*, 39-53.

Cai, L., Wang, J., Peng, J., Wu, Z., & Tan, X. (2018). Observation of the degradation of three types of plastic pellets exposed to UV irradiation in three different environments. *Science of the Total Environment*, 740-747.

California Coastal Commission's Water Quality Program. (2019, December). *CCA #40 Old Salinas River Estuary Critical Coastal Area*. Retrieved from California Coastal Commission: https://documents.coastal.ca.gov/assets/water-quality/ccc-factsheets/Central-Coast/CCA%2040%20Old%20Salinas%20River%20Estuary%20Factsheet%2012-16-19.pdf

Choy, C. A., Robison, B. H., Gagne, T. O., Erwin, B., Firl, E., Halden, R. U., . . . S. Van Houtan, K. (2019). The vertical distribution and biological transport of marine microplastics across the epipelagic and mesopelagic water column. *Scientific Reports*, 7843.

Chubarenko, I., Esiukova, E., Bagaev, A., Isachenko, I., Demchenko, N., Zobkov, M., . . . Khatmullina, L. (2018). Chapter 6: Behavior of Microplastics in Coastal Zones. In *Microplastic Contamination in Aquatic Environments* (pp. 175-223). Elsevier Inc.

Claessens, M., Van Cauwenberghe, L., Vandegehuchte, M. B., & Janssen, C. R. (2013). New techniques for the detection of microplastics in sediments and fieldcollected organisms. *Marine Pollution Bulletin*, 227-233.

CoastView. (2019, September 12). *Salinas River*. Retrieved from Coastview: https://coastview.org/articles/2019/09/12/salinas-river-castroville/

De Souza Machado, A. A., Lau, C. W., Kloas, W., Bergmann, J., Bachelier, J. B., Faltin, E., . . . Rillig, M. C. (2019). Microplastics Can Change Soil Properties and Affect Plant Performance. *Environmental Science and Technology*, 6044-6052.

Elkhorn Slough Foundation. (n.d.). *Property Profile Example*. Retrieved from Elkhorn Slough.

Eriksen, M., Lebreton, L. C., Carson, H. S., Thiel, M., Moore, C. J., Borerro, J. C., . . . Ryan, P. G. (2014). Plastic Pollution in the World ' s Oceans : More than 5 Trillion Plastic Pieces Weighing over 250 , 000 Tons Afloat at Sea. *PLOS One*, 1-15.

Fazey, F. M., & Ryan, P. G. (2016). Biofouling on buoyant marine plastics: An experimental study into the effect of size on surface longevity. *Environmental Pollution*, 354-360.

Free, C. M., Jensen, O. P., Mason, S. A., Eriksen, M., Williamson, N. J., & Boldgiv, B. (2014). High-levels of microplastic pollution in a large, remote, mountain lake. *Marine Pollution Bulletin*.

Gniadek, M., & Dąbrowska, A. (2019). The marine nano- and microplastics characterisation by SEM-EDX: The potential of the method in comparison with various physical and chemical approaches. *Marine Pollution Bulletin*, 210-216.

Hartmann, N. B., Hüffer, T., Thompson, R. C., Hassellöv, M., Verschoor, A., Daugaard, A. E., . . . Lusher, A. L. (2019). Are We Speaking the Same Language? Recommendations for a Definition and Categorization Framework for Plastic Debris. *Environmental Science and Technology*, 1039-1047.

Jansen, L., Henskens, M., & Hiemstra, F. (2019). *Report on use of plastics in agriculture.* Wageningen: Schuttelaar & Partners.

Jones, G. (2018, September 1). Recovering Agricultural Plastics: Obstacles and Opportunities. *Waste Advantage Magazine*.

Kole, P. J., Löhr, A. J., Belleghem, F. G., & Ragas, A. M. (2017). Wear and Tear of Tyres : A Stealthy Source of Microplastics in the Environment. *International Journal of Environmental Research and Public Health*, 1-31.

Law, K. (2017). Plastics in the Marine Environment. *Annual Review of Marine Science*, 205-229.

Lebreton, L. C., Van Der Zwet, J., Damsteeg, J. W., Slat, B., Andrady, A., & Reisser, J. (2017). River plastic emissions to the world's oceans. *Nature Communications*, 1-10.

Li, J., Liu, H., & Paul Chen, J. (2018). Microplastics in freshwater systems: A review on occurrence, environmental effects, and methods for microplastics detection. *Water Research*.

Lindon, J., Holmes, J., & Tranter, G. (2000). *Encyclopedia of Spectroscopy and Spectrometry: A-H.* United Kingdom: Academic Press.

MATLAB. (2018). *9.7.0.1190202 (R2019b)*. Natick, Massachusetts: The MathWorks Inc.

McLaughlin, K., Cade-Menun, B. J., & Paytan, A. (2006). The oxygen isotopic composition of phosphate in Elkhorn Slough, California: A tracer for phosphate sources. *Estuarine, Coastal and Shelf Science*, 499-506.

Mohamed Nor, N. H., & Obbard, J. P. (2014). Microplastics in Singapore's coastal mangrove ecosystems. *Marine Pollution Bulletin*, 278-283.

Moore, C. J. (2008). Synthetic polymers in the marine environment: A rapidly increasing, long-term threat. *Environmental Research*, 131-139.

Moss Landing Harbor District. (n.d.). *History*. Retrieved from Moss Landing Harbor: https://www.mosslandingharbor.dst.ca.us/about/history.htm

Newbury, D. E., Joy, D. C., Fiori, C. E., & Goldstein, J. I. (1986). *Advanced Scanning Electron Microscopy and X-Ray Microanalysis.* New York City: Springer.

Nizzetto, L., Futter, M., & Langaas, S. (2016). Are Agricultural Soils Dumps for Microplastics of Urban Origin? *Environmental Science and Technology*, 10777-10779.

Noren, F. (2007). *Small plastic particles in Coastal Swedish waters.* Lysekil: KIMO Sweden.

Rochman, C., Browne, M., Halpern, B., Hentschel, B., Hoh, E., Karapanagioti, H., . . . Thompson, R. (2013). Classify plastic waste as hazardous. *Nature*, 169-171.

Smith, R. E. (1973). *The hydrography of Elkhorn Slough: a shallow California coastal Eebayment: Annual Report, Part 2.* Moss Landing: Moss Landing Marine Laboratories.

Sullivan, L. (2022). Waste Land. New York , New York, USA.

Sutherland, B. R., Barrett, K. J., & Gingras, M. K. (2015). Clay settling in fresh and salt water. *Environmental Fluid Mechanics*, 147-160.

Sutton, R., Franz, A., Gilbreath, A., Lin, D., Miller, L., Sedlak, M., . . . Rochman, C. (2019). *Understanding Microplastic Levels, Pathways, and Transport in the San Francisco Bay Region.* Richmond: San Francisco Estuary Institute.

Thompson, R. C., Browne, M. A., & Galloway, T. S. (2010). Spatial Patterns of Plastic Debris along Estuarine Shorelines. *Environmental Science and Technology*, 3404-3409.

Thompson, R. C., Olson, Y., Mitchell, R. P., Davis, A., Rowland, S. J., John, A. W., . . . Russell, A. E. (2004). Lost at Sea: Where Is All the Plastic? *Science*, 838,304.

Van Cauwenberghe, L., & Janssen, C. R. (2014). Microplastics in bivalves cultured for human consumption. *Environmental Pollution*, 65-70.

Van Cauwenberghe, L., Vanreusel, A., Mees, J., & Janssen, C. R. (2013). Microplastic pollution in deep-sea sediments. *Environmental Pollution*, 495-499.

Vermeiren, P., Muñoz, C., & Ikejima, K. (2020). Microplastic identification and quantification from organic rich sediments: A validated laboratory protocol. *Environmental Pollution*, 262.

Weinstein, J. E., Crocker, B. K., & Gray, A. D. (2016). From macroplastic to microplastic: Degradation of high-density polyethylene, polypropylene, and polystyrene in a salt marsh habitat. *Environmental Toxicology and Chemistry*, 1632-1640.

Weithmann, N., Möller, J. N., Löder, M. G., Piehl, S., Laforsch, C., & Freitag, R. (2018). Organic fertilizer as a vehicle for the entry of microplastic into the environment. *Science Advances*, 1-7.

Whitmire, S. L., Bloem, S. J., & Toline, C. A. (2017). *Quantification of Microplastics on National Park Beaches NPS.* NOAA Marine Debris Program.

Yang, X., An, C., Feng, Q., Boufadel, M., & Ji, W. (2022). Aggregation of microplastics and clay particles in the nearshore environment: Characteristics, influencing factors, and implications. *Water Research*, 119077.

Yuan, G. L., Qin, J. X., Li, J., Lang, X. X., & Wang, G. H. (2014). Persistent organic pollutants in soil near the changwengluozha glacier of the central tibetan plateau, China: Their sorption to clays and implication. *Science of the Total Environment*, 309-315.

APPENDIX A

LIST OF MICROPLASTICS FOUND IN ORIGINAL THREE DENSITY SEPARATIONS

Site Name	Jar #	DS #	File Name	Color	Type	Length (mm)	Particle Count (total on 1 filter)	Particle Count (total in 50 g sediment)
Agriculture Site	1	1	AgSite1DS1001	black	fragment	0.0961		
	1	1	AgSite1DS1002	black	fragment	0.262		
	1	1	AgSite1DS1003	black	fragment	0.0601		
	1	1	AgSite1DS1004	black	fragment	0.0692		
	1	1	AgSite1DS1005	black	fragment	0.0641		
	1	1	AgSite1DS1006	blue	fragment	0.0915		
	1	1	AgSite1DS1007	black	fragment	0.0652		
	1	1	AgSite1DS1008	black	fragment	0.113		
	1	1	AgSite1DS1009	black	fragment	0.0627		
	1	1	AgSite1DS1010	black	fragment	0.0633		
	1	1	AgSite1DS1011	black	fragment	0.0882		
	1	1	AgSite1DS1012	black	fragment	0.0852		
	1	1	AgSite1DS1013	black	fragment	0.0863	13	
	1	2	AgSite1DS2001	black	fragment	0.206		
	1	2	AgSite1DS2002	black	fragment	0.0482		

	1	2	AgSite1DS2003	pink	fragment	0.0978		
	1	2	AgSite1DS2004	blue	fragment	0.184		
	1	2	AgSite1DS2005	black	fragment	0.0798		
	1	2	AgSite1DS2006	black	fragment	0.1	6	
	1	3	AgSite1DS3001	black	fragment	0.137		
	1	3	AgSite1DS3002	blue	fragment	0.0761		
	1	3	AgSite1DS3003	blue	fragment	0.079		
	1	3	AgSite1DS3004	black	fragment	0.0567		
	1	3	AgSite1DS3005	black	fragment	0.0726		
	1	3	AgSite1DS3006	black	fiber	1.5483		
	1	3	AgSite1DS3007	clear	fiber	2.2314		
	1	3		black	fragment	0.147	8	27
	1	1	AzevedoAg1DS1001	black	fragment	0.0661		
	1	1	AzevedoAg1DS1002	black	fragment	0.0881		
	1	1	AzevedoAg1DS1003	black	fiber	2.1049		
	1	1	AzevedoAg1DS1004	clear	fiber	1.453		
	1	1		black	fragment	0.208		
	1	1	AzevedoAg1DS1005	black	fragment	0.0845		
	1	1	AzevedoAg1DS1006	black	fragment	0.0642		
	1	1	AzevedoAg1DS1007	black	fragment	0.141	7	
	1	2	AzevedoAg1DS2001	blue	fragment	0.217		

	1	2	AzevedoAg1DS2002	black	fragment	0.0613		
	1	2	AzevedoAg1DS2003	black	fragment	0.111		
	1	2	AzevedoAg1DS2004	black	fragment	0.0441		
	1	2	AzevedoAg1DS2005	blue	fragment	0.603		
	1	2	AzevedoAg1DS2006	black	fragment	0.104		
	1	2	AzevedoAg1DS2007	black	fragment	0.0481		
	1	2	AzevedoAg1DS2008	black	fragment	0.0601		
	1	2	AzevedoAg1DS2009	blue	fragment	0.0426		
	1	2	AzevedoAg1DS2010	black	fragment	0.0426		
	1	2	AzevedoAg1DS2011	blue	fragment	0.0945		
	1	2	AzevedoAg1DS2012	black	fragment	0.032		
	1	2	AzevedoAg1DS2013	blue	fragment	0.0481		
	1	2	AzevedoAg1DS2014	black	fragment	0.0762		
	1	2	AzevedoAg1DS2015	black	fragment	0.0401		
	1	2	AzevedoAg1DS2016	black	fragment	0.0633		
	1	2	AzevedoAg1DS2017	red	fiber	1.2756		
	1	2	AzevedoAg1DS2018	black	fragment	0.0345		
	1	2	AzevedoAg1DS2019	blue	fragment	0.171		
	1	2	AzevedoAg1DS2020	black	fragment	0.0481		
	1	2		pink	Fragment	0.0361	21	
	1	3	AzevedoAg1DS3001	green	fragment	0.143		

	1	3	AzevedoAg1DS3002	blue	fiber	0.1695		
	1	3	AzevedoAg1DS3003	blue	fragment	0.0694		
	1	3	AzevedoAg1DS3004	clear	fiber	0.454		
	1	3	AzevedoAg1DS3005	black	fragment	0.0602		
	1	3	AzevedoAg1DS3006	black	fiber	1.1013		
	1	3	AzevedoAg1DS3007	black	fragment	0.0515		
	1	3	AzevedoAg1DS3008	black	fragment	0.0383		
	1	3	AzevedoAg1DS3009	black	fragment	0.0309		
	1	3	AzevedoAg1DS3010	black	fragment	0.0644		
	1	3	AzevedoAg1DS3011	black	fragment	0.0602		
	1	3	AzevedoAg1DS3012	black	fragment	0.0698		
	1	3	AzevedoAg1DS3013	black	fragment	0.0452		
	1	3	AzevedoAg1DS3014	black	fragment	0.217		
	1	3	AzevedoAg1DS3015	black	fragment	0.21		
	1	3	AzevedoAg1DS3016	black	fragment	0.0727	16	37
	2	1	AzevedoAg2DS1001	black	fiber	0.5781	1	
	2	2	AzevedoAg2DS2001	blue	fragment	0.545		
	2	2	AzevedoAg2DS2002	black	fragment	0.11		
	2	2	AzevedoAg2DS2003	black	fragment	0.0922		
	2	2	AzevedoAg2DS2004	blue	fragment	0.179		
	2	2		black	fragment	0.0395		

	2	2	AzevedoAg2DS2005	black	fragment	0.0527		
	2	2	AzevedoAg2DS2006	blue	fragment	0.061	7	
	2	3	AzevedoAg2DS3001	black	fragment	0.0395		
	2	3	AzevedoAg2DS3002	black	fragment	0.0283		
	2	3		black	fragment	0.033		
	2	3	AzevedoAg2DS3003	black	fragment	0.0361		
	2	3	AzevedoAg2DS3004	black	fragment	0.0441		
	2	3	AzevedoAg2DS3005	blue	fiber	2.2916	6	14
	3	1	AzevedoAg3DS1001	black	Fragment	0.108		
	3	1	AzevedoAg3DS1002	black	fragment	0.597		
	3	1	AzevedoAg3DS1003	black	fragment	0.259		
	3	1	AzevedoAg3DS1004	black	fragment	0.0903		
	3	1	AzevedoAg3DS1005	black	fragment	0.0531		
	3	1	AzevedoAg3DS1006	black	fragment	0.0915		
	3	1	AzevedoAg3DS1007	black	fragment	0.109		
	3	1	AzevedoAg3DS1008	black	fragment	0.199		
	3	1	AzevedoAg3DS1009	black	fragment	0.0533		
	3	1	AzevedoAg3DS1010	black	fragment	0.0565	10	
	3	2	AzevedoAg3DS2001	blue	fragment	0.0879		
	3	2	AzevedoAg3DS2002	black	fragment	0.033		
	3	2	AzevedoAg3DS2003	black	fragment	0.081		

	3	2	AzevedoAg3DS2004	black	fragment	0.0626		
	3	2	AzevedoAg3DS2005	black	fragment	0.0721		
	3	2	AzevedoAg3DS2006	black	fragment	0.0856		
	3	2	AzevedoAg3DS2007	black	fragment	0.0441		
	3	2	AzevedoAg3DS2008	black	fragment	0.0778		
	3	2	AzevedoAg3DS2009	black	fragment	0.0682	9	
	3	3	AzevedoAg3DS3001	black	fragment	0.227		
	3	3	AzevedoAg3DS3002	black	fragment	0.173		
	3	3	AzevedoAg3DS3003	black	fragment	0.0593		
	3	3	AzevedoAg3DS3004	black	fiber	1.1519		
	3	3	AzevedoAg3DS3005	black	fragment	0.0653		
	3	3	AzevedoAg3DS3006	black	fiber	1.3427		
	3	3	AzevedoAg3DS3007	black	fiber	1.6011		
	3	3	AzevedoAg3DS3008	blue	fiber	0.302		
	3	3	AzevedoAg3DS3009	black	fragment	0.0478		
	3	3	AzevedoAg3DS3010	blue	fiber	0.141		
	3	3	AzevedoAg3DS3011	blue	fiber	1.15	11	30
Azevedo	1	1	Azevedo1RedoDS1001	black	fragment	0.106		
	1	1	Azevedo1RedoDS1002	black	fragment	0.0596		
	1	1	Azevedo1RedoDS1003	black	fragment	0.0361		
	1	1	Azevedo1RedoDS1004	black	fragment	0.0611	4	

	1	2	Azevedo1RedoDS2001	black	fragment	0.0841		
	1	2	Azevedo1RedoDS2002	black	fragment	0.0561	2	
	1	3	Azevedo1RedoDS3001	blue	fragment	0.391		
	1	3	Azevedo1RedoDS3002	black	fragment	0.0401		
	1	3	Azevedo1RedoDS3003	black	fragment	0.0431		
	1	3		blue	fragment	0.0642		
	1	3	Azevedo1RedoDS3004	black	fragment	0.0409		
	1	3	Azevedo1RedoDS3005	black	fragment	0.032		
	1	3	Azevedo1RedoDS3006	red	fiber	0.16		
	1	3	Azevedo1RedoDS3007	black	fragment	0.0283		
	1	3	Azevedo1RedoDS3008	blue	fragment	0.1		
	1	3	Azevedo1RedoDS3009	blue	fragment	1.1		
	1	3	Azevedo1RedoDS3010	blue	fragment	0.0856		
	1	3	Azevedo1RedoDS3011	black	fragment	0.0496		
	1	3	Azevedo1RedoDS3012	black	fragment	0.032		
	1	3	Azevedo1RedoDS3013	black	fragment	0.0457		
	1	3	Azevedo1RedoDS3014	black	fragment	0.09		
	1	3	Azevedo1RedoDS3015	black	fragment	0.0562		
	1	3	Azevedo1RedoDS3016	black	fragment	0.0748		
	1	3	Azevedo1RedoDS3017	black	fiber	0.1264		
	1	3		blue	fragment	0.0761		
	1	3	Azevedo1RedoDS3018	blue	fragment	0.0795		
	1	3	Azevedo1RedoDS3019	blue	fiber	0.437	21	**27**

	2	1	Azevedo2RedoDS1001	blue	fragment	0.589		
	2	1	Azevedo2RedoDS1002	black	fragment	0.0481		
	2	1	Azevedo2RedoDS1003	black	fragment	0.273		
	2	1	Azevedo2RedoDS1004	black	fragment	0.0484	4	
	2	2	Azevedo2RedoDS2001	black	fragment	0.028		
	2	2	Azevedo2RedoDS2002	black	fiber	0.4687		
	2	2	Azevedo2RedoDS2003	blue	fragment	0.0793		
	2	2	Azevedo2RedoDS2004	blue	fragment	0.0481		
	2	2		black	fragment	0.18		
	2	2	Azevedo2RedoDS2005	blue	fiber	0.185	6	
	2	3	Azevedo2RedoDS3001	blue	fiber	0.4959		
	2	3	Azevedo2RedoDS3002	black	fragment	0.106		
	2	3		black	fragment	0.034		
	2	3	Azevedo2RedoDS3003	clear	fragment	1.24		
	2	3	Azevedo2RedoDS3004	black	fiber	0.4676		
	3	3	Azevedo2RedoDS3005	black	fragment	0.0537	6	**16**
	3	1	Azevedo3RedoDS1001	black	fragment	0.0361		
	3	1	Azevedo3RedoDS1002	black	fragment	0.0652		
	3	1	Azevedo3RedoDS1003	black	fragment	0.028		
	3	1	Azevedo3RedoDS1004	black	fiber	0.0557		
	3	1	Azevedo3RedoDS1005	black	fragment	0.024		
	3	1	Azevedo3RedoDS1006	black	fragment	0.0401	6	
	3	2	Azevedo3RedoDS2001	black	fragment	0.0448		

	3	2	Azevedo3RedoDS2002	black	fragment	0.0401		
	3	2	Azevedo3RedoDS2003	black	fragment	0.051		
	3	2	Azevedo3RedoDS2004	black	fragment	0.0574		
	3	2	Azevedo3RedoDS2005	pink	Fragment	0.0623		
	3	2	Azevedo3RedoDS2006	black	fragment	0.028	6	
	3	3	Azevedo3RedoDS3001	black	fragment	0.032		
	3	3	Azevedo3RedoDS3002	black	fragment	0.0736		
	3	3	Azevedo3RedoDS3003	black	fragment	0.0401		
	3	3	Azevedo3RedoDS3004	black	fragment	0.0403		
	3	3	Azevedo3RedoDS3005	black	fragment	0.0513		
	3	3	Azevedo3RedoDS3006	black	fragment	0.0539		
	3	3	Azevedo3RedoDS3007	black	fragment	0.0457	7	**19**
	4	1	Azevedo4RedoDS1001	black	fragment	0.159		
	4	1	Azevedo4RedoDS1002	black	fragment	0.1		
	4	1	Azevedo4RedoDS1003	black	fragment	0.0562		
	4	1	Azevedo4RedoDS1004	black	fragment	0.0342		
	4	1	Azevedo4RedoDS1005	black	fragment	0.112		
	4	1		black	fragment	0.0412		
	4	1	Azevedo4RedoDS1006	black	fragment	0.0481		
	4	1	Azevedo4RedoDS1007	black	fragment	0.0521	8	
	4	2	Azevedo4RedoDS2001	blue	fragment	0.0748		
	4	2	Azevedo4RedoDS2002	blue	fragment	0.086		
	4	2	Azevedo4RedoDS2003	black	fragment	0.155		

	4	2	Azevedo4RedoDS2004	blue	fragment	0.0774		
	4	2	Azevedo4RedoDS2005	blue	fragment	0.0552		
	4	2	Azevedo4RedoDS2006	blue	fragment	0.0583		
	4	2	Azevedo4RedoDS2007	blue	fragment	0.156		
	4	2	Azevedo4RedoDS2008	black	fragment	0.0561		
	4	2	Azevedo4RedoDS2009	black	fragment	0.0482		
	4	2		black	fragment	0.0363		
	4	2	Azevedo4RedoDS2010	black	fragment	0.0739		
	4	2	Azevedo4RedoDS2011	red	fiber	0.8561		
	4	2	Azevedo4RedoDS2012	black	fragment	0.0663		
	4	2	Azevedo4RedoDS2013	black	fragment	0.0646		
	4	2	Azevedo4RedoDS2014	black	fiber	0.112		
	4	2	Azevedo4RedoDS2015	black	fragment	0.0401	16	
	4	3	Azevedo4RedoDS3001	black	fragment	0.0562		
	4	3	Azevedo4RedoDS3002	blue	fragment	0.0453		
	4	3	Azevedo4RedoDS3003	black	fiber	0.104		
	4	3	Azevedo4RedoDS3004	black	fragment	0.0361		
	4	3	Azevedo4RedoDS3005	black	fiber	0.543		
	4	3	Azevedo4RedoDS3006	blue	fragment	0.15		
	4	3	Azevedo4RedoDS3007	black	fragment	0.0574		
	4	3	Azevedo4RedoDS3008	blue	fragment	0.0539		
	4	3	Azevedo4RedoDS3009	blue	fragment	0.0567		
	4	3	Azevedo4RedoDS3010	black	fragment	0.0558		

	4	3	Azevedo4RedoDS3011	black	fragment	0.0652	11	35
Bird	1	1	Bird1DS1001	black	fragment	0.0701		
	1	1		black	fragment	0.0722		
	1	1	Bird1DS1002	black	fragment	0.0426		
	1	1		black	fragment	0.0378		
	1	1	Bird1DS1003	black	fragment	0.0481		
	1	1		black	fragment	0.085		
	1	1	Bird1DS1004	black	fragment	0.0481		
	1	1	Bird1DS1005	black	fragment	0.0409		
	1	1	Bird1DS1006	black	fiber	1.1583		
	1	1	Bird1DS1007	black	fragment	0.0596		
	1	1	Bird1DS1008	black	fragment	0.0482		
	1	1	Bird1DS1009	black	fiber	0.0806		
	1	1	Bird1DS1010	black	fragment	0.0431		
	1	1	Bird1DS1011	black	fragment	0.0481		
	1	1	Bird1DS1012	black	fragment	0.0521		
	1	1	Bird1DS1013	black	fragment	0.0441		
	1	1	Bird1DS1014	black	fragment	0.0667		
	1	1	Bird1DS1015	black	fragment	0.0481		
	1	1	Bird1DS1016	black	fragment	0.0681		
	1	1	Bird1DS1017	black	fragment	0.0484		
	1	1	Bird1DS1018	black	fragment	0.0817		
	1	1		black	fragment	0.0778		

	1	1	Bird1DS1019	black	Fragment	0.068		
	1	1	Bird1DS1020	black	fragment	0.0522		
	1	1	Bird1DS1021	black	fragment	0.0646		
	1	1	Bird1DS1022	black	fragment	0.0801		
	1	1	Bird1DS1023	black	fragment	0.142		
	1	1	Bird1DS1024	black	fiber	0.117		
	1	1		black	fragment	0.0482		
	1	1	Bird1DS1025	black	fragment	0.0709		
	1	1	Bird1DS1026	black	fragment	0.0771		
	1	1	Bird1DS1027	black	fragment	0.0836	32	
	1	2	Bird1DS2001	black	fragment	0.0601		
	1	2		black	fragment	0.032		
	1	2	Bird1DS2002	black	fragment	0.0481		
	1	2		black	fragment	0.0481		
	1	2		black	fragment	0.0689		
	1	2	Bird1DS2003	black	fragment	0.0562		
	1	2	Bird1DS2004	black	fragment	0.0545		
	1	2	Bird1DS2005	blue	fragment	0.0641		
	1	2	Bird1DS2006	black	fragment	0.0602		
	1	2	Bird1DS2007	black	fragment	0.0521		
	1	2		black	fragment	0.0481		
	1	2	Bird1DS2008	black	fragment	0.0561		
	1	2	Bird1DS2009	black	fragment	0.0626		

	1	2		black	fragment	0.032		
	1	2	Bird1DS2010	black	fragment	0.0646		
	1	2	Bird1DS2011	blue	fragment	0.0441		
	1	2		black	fragment	0.0567		
	1	2		black	fragment	0.101		
	1	2		black	fragment	0.0433		
	1	2	Bird1DS2012	clear	fiber	0.9955		
	1	2	Bird1DS2013	black	fiber	1.2029		
	1	2		black	fiber	0.0545		
	1	2		black	fiber	0.108	23	
	1	3	Bird1DS3001	black	fragment	0.14		
	1	3		blue	fragment	0.0817		
	1	3	Bird1DS3002	black	fragment	0.0804		
	1	3	Bird1DS3003	gray	fiber	0.191		
	1	3	Bird1DS3004	black	fragment	0.0494		
	1	3		black	fragment	0.0599		
	1	3	Bird1DS3005	black	fragment	0.0642		
	1	3	Bird1DS3006	black	fragment	0.0885		
	1	3		black	fragment	0.0388		
	1	3	Bird1DS3007	black	fragment	0.0765		
	1	3	Bird1DS3008	black	fragment	0.0569		
	1	3	Bird1DS3009	black	fragment	0.0673		
	1	3	Bird1DS3010	black	fragment	0.0896		

	1	3	Bird1DS3011	black	fragment	0.108		
	1	3	Bird1DS3012	black	fragment	0.0847		
	1	3	Bird1DS3013	black	fragment	0.112		
	1	3	Bird1DS3014	black	fragment	0.0655		
	1	3	Bird1DS3015	black	fragment	0.0632		
	1	3	Bird1DS3016	black	fragment	0.0739		
	1	3		black	fragment	0.0651		
	1	3		black	fragment	0.0867		
	1	3	Bird1DS3017	black	fragment	0.145		
	1	3	Bird1DS3018	black	fragment	0.258		
	1	3	Bird1DS3019	black	fragment	0.145	24	**79**
	2	1	Bird2DS1001	black	fragment	0.116		
	2	1	Bird2DS1002	black	fragment	0.0502		
	2	1	Bird2DS1003	black	fragment	0.0778		
	2	1	Bird2DS1004	black	fiber	0.0881		
	2	1	Bird2DS1005	black	fragment	0.0453		
	2	1	Bird2DS1006	black	fragment	0.0513		
	2	1	Bird2DS1007	black	fragment	0.0578		
	2	1	Bird2DS1008	black	fragment	0.0448		
	2	1	Bird2DS1009	black	fragment	0.0914		
	2	1	Bird2DS1010	black	fragment	0.0522		
	2	1	Bird2DS1011	black	fragment	0.0467		
	2	1		black	fragment	0.0361		

	2	1	Bird2DS1012	black	fragment	0.0482		
	2	1	Bird2DS1013	black	fragment	0.0896	14	
	2	2	Bird2DS2001	black	fragment	0.0657		
	2	2	Bird2DS2002	black	fiber	0.0686		
	2	2	Bird2DS2003	black	fiber	0.0601		
	2	2	Bird2DS2004	black	fragment	0.0441		
	2	2	Bird2DS2005	black	fragment	0.0562		
	2	2	Bird2DS2006	black	fragment	0.0521		
	2	2	Bird2DS2007	pink	Fragment	0.0521		
	2	2		black	fragment	0.0401		
	2	2	Bird2DS2008	black	fragment	0.032		
	2	2	Bird2DS2009	black	fragment	0.0433		
	2	2	Bird2DS2010	black	fragment	0.0502		
	2	2	Bird2DS2011	black	fragment	0.0765		
	2	2		black	fragment	0.0401		
	2	2	Bird2DS2012	black	fragment	0.0481		
	2	2	Bird2DS2013	black	fragment	0.0401		
	2	2	Bird2DS2014	black	fragment	0.0721		
	2	2	Bird2DS2015	black	fragment	0.0561		
	2	2	Bird2DS2016	black	Fragment	0.0361		
	2	2		black	Fragment	0.0378		
	2	2		black	fragment	0.0412		
	2	2	Bird2DS2017	black	fragment	0.0401		

	2	2	Bird2DS2018	black	fragment	0.0521		
	2	2	Bird2DS2019	black	fragment	0.0409		
	2	2	Bird2DS2020	black	fragment	0.18		
	2	2	Bird2DS2021	black	fragment	0.0626		
	2	2	Bird2DS2022	black	fragment	0.101	26	
	2	3	Bird2DS3001	blue	fiber	0.4211		
	2	3	Bird2DS3002	black	fiber	0.8366		
	2	3	Bird2DS3003	blue	fiber	1.0733		
	2	3	Bird2DS3004	black	fiber	1.0436		
	2	3	Bird2DS3005	black	fragment	0.108		
	2	3	Bird2DS3006	black	fragment	0.0595		
	2	3	Bird2DS3007	black	fragment	0.0606		
	2	3	Bird2DS3008	black	fragment	0.0571		
	2	3	Bird2DS3009	black	fragment	0.107		
	2	3	Bird2DS3010	black	fragment	0.0424		
	2	3	Bird2DS3011	black	fragment	0.0401		
	2	3	Bird2DS3012	black	fragment	0.134		
	2	3	Bird2DS3013	black	fragment	0.0566		
	2	3		black	fragment	0.0698		
	2	3		black	fragment	0.0615		
	2	3		black	fragment	0.0381		
	2	3		black	fragment	0.059	17	**57**
	3	1	Bird3DS1001	blue	fragment	0.0736		

	3	1	Bird3DS1002	black	fragment	0.0678		
	3	1	Bird3DS1003	black	fragment	0.0514		
	3	1	Bird3DS1004	black	fragment	0.0383		
	3	1	Bird3DS1005	black	fragment	0.0984		
	3	1	Bird3DS1006	black	fragment	0.145		
	3	1	Bird3DS1007	black	fiber	0.8391		
	3	1	Bird3DS1008	black	fragment	0.067		
	3	1	Bird3DS1009	blue	fragment	0.0538		
	3	1	Bird3DS1010	black	fragment	0.0944		
	3	1		black	fragment	0.0338		
	3	1	Bird3DS1011	black	fragment	0.0663		
	3	1	Bird3DS1012	black	fragment	0.0753		
	3	1	Bird3DS1013	black	fragment	0.0597		
	3	1	Bird3DS1014	black	fragment	0.108		
	3	1	Bird3DS1015	black	fragment	0.0365		
	3	1	Bird3DS1016	black	fragment	0.0472		
	3	1	Bird3DS1017	blue	fragment	0.05		
	3	1		black	fragment	0.108		
	3	1	Bird3DS1018	black	Fragment	0.046		
	3	1	Bird3DS1019	black	fragment	0.0622	21	
	3	2	Bird3DS2001	blue	fiber	0.0461		
	3	2	Bird3DS2002	blue	fiber	0.439		
	3	2	Bird3DS2003	black	fragment	0.0807		

	3	2	Bird3DS2004	black	fragment	0.0316		
	3	2		black	fragment	0.0314		
	3	2	Bird3DS2005	black	fragment	0.0489		
	3	2	Bird3DS2006	black	fragment	0.04		
	3	2		black	fragment	0.0494		
	3	2	Bird3DS2007	black	fragment	0.0577		
	3	2	Bird3DS2008	blue	fragment	0.0461		
	3	2	Bird3DS2009	black	fragment	0.0454		
	3	2		black	fragment	0.0461	12	
	3	3	Bird3DS3001	black	fragment	0.0974		
	3	3		black	fragment	0.114		
	3	3		black	fragment	0.111		
	3	3	Bird3DS3002	black	fragment	0.0623		
	3	3		blue	fragment	0.0851		
	3	3	Bird3DS3003	green	fragment	0.105		
	3	3	Bird3DS3004	black	fragment	0.11	7	**40**
	4	1	Bird4DS1001	black	fragment	0.0896		
	4	1	Bird4DS1002	black	fragment	0.0823		
	4	1	Bird4DS1003	black	fragment	0.0585		
	4	1	Bird4DS1004	black	fragment	0.0926		
	4	1	Bird4DS1005	black	fragment	0.0971		
	4	1	Bird4DS1006	black	fragment	0.0578		
	4	1	Bird4DS1007	black	Fragment	0.0351		

	4	1	Bird4DS1008	black	fragment	0.0521	8	
	4	2	Bird4DS2001	black	fragment	0.112		
	4	2		black	fragment	0.134		
	4	2	Bird4DS2002	black	fragment	0.0935		
	4	2	Bird4DS2003	black	fragment	0.0671		
	4	2	Bird4DS2004	black	fragment	0.155		
	4	2	Bird4DS2005	black	fragment	0.0965		
	4	2	Bird4DS2006	black	fragment	0.0388		
	4	2	Bird4DS2007	black	fragment	0.0664		
	4	2	Bird4DS2008	black	fragment	0.0389		
	4	2		black	fragment	0.0403		
	4	2	Bird4DS2009	black	fragment	0.0526		
	4	2		black	fragment	0.042		
	4	2	Bird4DS2010	black	fragment	0.112		
	4	2		blue	fragment	0.0613	14	
	4	3	Bird4DS3001	black	fragment	0.0637		
	4	3	Bird4DS3002	blue	fragment	0.0691		
	4	3	Bird4DS3003	black	fragment	0.0401		
	4	3	Bird4DS3004	pink	Fragment	0.0388		
	4	3	Bird4DS3005	black	fragment	0.0678		
	4	3	Bird4DS3006	black	fragment	0.0445		
	4	3		black	fragment	0.046		
	4	3	Bird4DS3007	black	fragment	0.0576	8	**30**

Hester	1	1	Hester1RedoDS1001	black	fragment	0.0656		
	1	1	Hester1RedoDS1002	black	fiber	0.3879		
	1	1	Hester1RedoDS1003	black	fragment	0.0426		
	1	1	Hester1RedoDS1004	black	fragment	0.0466		
	1	1	Hester1RedoDS1005	black	fragment	0.0466		
	1	1	Hester1RedoDS1006	black	fragment	0.0429		
	1	1		black	fragment	0.0444		
	1	1	Hester1RedoDS1007	black	Fragment	0.0588		
	1	1	Hester1RedoDS1008	black	fragment	0.0376		
	1	1	Hester1RedoDS1010	black	fragment	0.102		
	1	1		black	fragment	0.0542		
	1	1	Hester1RedoDS1011	black	fiber	0.217		
	1	1	Hester1RedoDS1012	black	fragment	0.13	13	
	1	2	Hester1RedoDS2001	red	fiber	1.3762		
	1	2	Hester1RedoDS2002	black	Fragment	0.101		
	1	2	Hester1RedoDS2003	black	fragment	0.0573		
	1	2	Hester1RedoDS2004	black	fragment	0.0526		
	1	2	Hester1RedoDS2005	black	fragment	0.0474		
	1	2	Hester1RedoDS2006	pink	Fragment	0.0426		
	1	2	Hester1RedoDS2007	black	fragment	0.0551		
	1	2	Hester1RedoDS2008	black	fragment	0.0393		

	1	2	Hester1RedoDS2009	black	fragment	0.0958		
	1	2	Hester1RedoDS2010	black	fragment	0.0751	10	
	1	3	Hester1RedoDS3001	black	fragment	0.0724		
	1	3	Hester1RedoDS3002	black	fiber	0.0639		
	1	3		pink	Fragment	0.0339		
	1	3	Hester1RedoDS3003	black	fragment	0.0678		
	1	3	Hester1RedoDS3004	black	fragment	0.0608		
	1	3	Hester1RedoDS3005	black	fragment	0.0459		
	1	3	Hester1RedoDS3006	pink	Fragment	0.0497		
	1	3	Hester1RedoDS3007	black	fragment	0.0727		
	1	3	Hester1RedoDS3008	black	fragment	0.0613		
	1	3	Hester1RedoDS3009	black	fragment	0.0849		
	1	3		black	fragment	0.0551		
	1	3	Hester1RedoDS3010	black	Fragment	0.0589		
	1	3	Hester1RedoDS3011	black	Fragment	0.0491	13	**36**
	2	1	Hester2RedoDS1001	black	fragment	0.0401		
	2	1		blue	fragment	0.0739		
	2	1	Hester2RedoDS1002	black	fragment	0.084		
	2	1	Hester2RedoDS1003	black	fragment	0.0983		
	2	1	Hester2RedoDS1004	black	fragment	0.0547		
	2	1	Hester2RedoDS1005	black	fragment	0.137		

	2	1	Hester2RedoDS1006	black	fragment	0.0471		
	2	1	Hester2RedoDS1007	black	fragment	0.0401		
	2	1	Hester2RedoDS1008	black	fragment	0.0809	9	
	2	2	Hester2RedoDS2001	black	fiber	0.419		
	2	2	Hester2RedoDS2002	black	fragment	0.0638		
	2	2		black	fragment	0.105		
	2	2	Hester2RedoDS2003	black	Fragment	0.0559		
	2	2	Hester2RedoDS2004	black	fragment	0.0754		
	2	2	Hester2RedoDS2005	black	fiber	0.0283		
	2	2	Hester2RedoDS2006	black	fragment	0.0933		
	2	2	Hester2RedoDS2007	black	fragment	0.0488		
	2	2	Hester2RedoDS2008	black	fragment	0.164		
	2	2	Hester2RedoDS2009	black	fragment	0.0655		
	2	2	Hester2RedoDS2010	black	fragment	0.096		
	2	2	Hester2RedoDS2011	black	fragment	0.0363		
	2	2	Hester2RedoDS2012	black	Fragment	0.0388		
	2	2	Hester2RedoDS2013	black	Fragment	0.0665		
	2	2	Hester2RedoDS2014	black	fragment	0.0717		
	2	2	Hester2RedoDS2015	black	fiber	0.1114	16	
	2	3	Hester2RedoDS3002	black	Fragment	0.0626		
	2	3	Hester2RedoDS3003	black	fragment	0.0601		

	2	3	Hester2RedoDS3004	black	fragment	0.0899	3	28
	3	1	Hester3RedoDS1001	black	fragment	0.0311		
	3	1		black	fragment	0.0251		
	3	1	Hester3RedoDS1002	black	fragment	0.0647		
	3	1	Hester3RedoDS1003	black	fragment	0.0366		
	3	1	Hester3RedoDS1004	green	fragment	0.192		
	3	1	Hester3RedoDS1005	green	fragment	0.068		
	3	1	Hester3RedoDS1006	black	fragment	0.0277		
	3	1	Hester3RedoDS1007	black	fragment	0.0452		
	3	1	Hester3RedoDS1008	black	fragment	0.0309		
	3	1	Hester3RedoDS1009	blue	fiber	0.1775		
	3	1	Hester3RedoDS1010	green	fragment	0.0619		
	3	1	Hester3RedoDS1011	green	fragment	0.0389		
	3	1	Hester3RedoDS1012	green	fragment	0.066		
	3	1	Hester3RedoDS1013	blue	fiber	0.143		
	3	1	Hester3RedoDS1014	black	fragment	0.0899		
	3	1	Hester3RedoDS1015	black	fragment	0.0314	16	
	3	2	Hester3RedoDS2001	blue	fragment	0.0563		
	3	2		clear	fragment	0.107		
	3	2	Hester3RedoDS2002	blue	fragment	0.0338		
	3	2	Hester3RedoDS2003	black	fragment	0.0492		

	3	2	Hester3RedoDS2004	black	fragment	0.0465		
	3	2	Hester3RedoDS2005	black	fragment	0.0862		
	3	2	Hester3RedoDS2006	black	fragment	0.0378		
	3	2	Hester3RedoDS2007	black	Fragment	0.0556		
	3	2	Hester3RedoDS2008	black	fiber	0.1049		
	3	2	Hester3RedoDS2009	black	fragment	0.0442		
	3	2	Hester3RedoDS2010	black	fragment	0.0443		
	3	2	Hester3RedoDS2011	black	fragment	0.0611		
	3	2		black	fragment	0.0391		
	3	2	Hester3RedoDS2012	black	fragment	0.0622		
	3	2	Hester3RedoDS2013	black	fragment	0.0488		
	3	2	Hester3RedoDS2014	black	fragment	0.0363		
	3	2	Hester3RedoDS2015	black	Fragment	0.0388		
	3	2	Hester3RedoDS2016	green	fragment	0.0972		
	3	2	Hester3RedoDS2017	black	fiber	0.074		
	3	2	Hester3RedoDS2018	black	fragment	0.0455		
	3	2	Hester3RedoDS2019	black	fiber	0.0683		
	3	2	Hester3RedoDS2020	green	fragment	0.108		
	3	2	Hester3RedoDS2021	black	fragment	0.0679	23	
	3	3	Hester3RedoDS3001	black	fragment	0.194		
	3	3	Hester3RedoDS3002	black	fragment	0.0513		

	3	3		black	fragment	0.068		
	3	3	Hester3RedoDS3003	black	fiber	0.0482		
	3	3		black	fragment	0.0402		
	3	3	Hester3RedoDS3004	black	fragment	0.0632		
	3	3	Hester3RedoDS3005	black	fiber	0.031		
	3	3		black	fragment	0.0356		
	3	3	Hester3RedoDS3006	black	fragment	0.0443		
	3	3	Hester3RedoDS3007	black	fragment	0.0321		
	3	3	Hester3RedoDS3008	blue	fragment	0.0389		
	3	3	Hester3RedoDS3009	clear	fragment	0.184		
	3	3	Hester3RedoDS3010	black	fragment	0.0493		
	3	3	Hester3RedoDS3011	black	fragment	0.0589		
	3	3	Hester3RedoDS3012	black	fragment	0.0516		
	3	3	Hester3RedoDS3013	black	fragment	0.0455		
	3	3		black	fragment	0.0303		
	3	3	Hester3RedoDS3014	clear	fragment	0.0676		
	3	3	Hester3RedoDS3015	black	fragment	0.0507		
	3	3	Hester3RedoDS3016	black	fragment	0.0478		
	3	3	Hester3RedoDS3017	black	fragment	0.0402		
	3	3	Hester3RedoDS3018	black	fragment	0.0451		
	3	3	Hester3RedoDS3019	black	fragment	0.0772		

	3	3	Hester3RedoDS3020	black	fiber	0.02527	24	**63**
	4	1	Hester4RedoDS1001	black	fiber	1.9704		
	4	1	Hester4RedoDS1002	black	fiber	0.6228		
	4	1	Hester4RedoDS1003	black	fragment	0.0541		
	4	1	Hester4RedoDS1004	blue	fragment	0.0356	4	
	4	2	Hester4RedoDS2001	black	fragment	0.0446		
	4	2	Hester4RedoDS2002	black	fragment	0.0651		
	4	2	Hester4RedoDS2003	black	fragment	0.168		
	4	2		black	fragment	0.0478		
	4	2	Hester4RedoDS2004	black	Fragment	0.0601		
	4	2	Hester4RedoDS2005	black	fragment	0.1		
	4	2	Hester4RedoDS2006	black	fragment	0.0401		
	4	2	Hester4RedoDS2007	black	fragment	0.0628	8	
	4	3	Hester4RedoDS3001	black	fragment	0.0461		
	4	3	Hester4RedoDS3002	black	fragment	0.0865		
	4	3	Hester4RedoDS3003	black	fragment	0.0516	3	**15**
	1	1	SealBend1RedoDS1001	green	fragment	0.0481		
	1	1	SealBend1RedoDS1002	blue	fragment	0.0646		
	1	1	SealBend1RedoDS1003	black	fragment	0.0561		
	1	1	SealBend1RedoDS1004	black	fragment	0.0361		
	1	1	SealBend1RedoDS1005	black	fragment	0.028		

	1	1		black	fragment	0.024		
	1	1		black	fragment	0.024		
	1	1		black	fragment	0.024		
Seal Bend	1	1	SealBend1RedoDS1006	blue	fiber	0.496		
	1	1	SealBend1RedoDS1007	black	fragment	0.176		
	1	1	SealBend1RedoDS1008	black	fragment	0.0489		
	1	1	SealBend1RedoDS1009	black	fragment	0.0601		
	1	1	SealBend1RedoDS1010	black	fragment	0.0726	13	
	1	2	SealBend1RedoDS2001	black	fiber	0.0879		
	1	2	SealBend1RedoDS2002	black	fiber	0.0885		
	1	2	SealBend1RedoDS2003	black	fragment	0.0602		
	1	2	SealBend1RedoDS2004	black	fragment	0.0904		
	1	2	SealBend1RedoDS2005	black	fragment	0.236		
	1	2	SealBend1RedoDS2006	black	fragment	0.0761		
	1	2		blue	fragment	0.032		
	1	2	SealBend1RedoDS2007	black	fiber	0.0689		
	1	2	SealBend1RedoDS2008	black	fragment	0.0722		
	1	2	SealBend1RedoDS2009	black	fragment	0.0642		
	1	2		black	fragment	0.0646		
	1	2	SealBend1RedoDS2010	black	fiber	0.1294	12	
	1	3	SealBend1RedoDS3001	black	fragment	0.0583		

	1	3		black	fragment	0.0521			
	1	3	SealBend1RedoDS3002	black	fiber	0.0537			
	1	3	SealBend1RedoDS3003	black	fragment	0.121			
	1	3	SealBend1RedoDS3004	blue	fragment	0.032			
	1	3	SealBend1RedoDS3005	black	fragment	0.0646			
	1	3		black	fragment	0.0601			
	1	3		black	fragment	0.0481			
	1	3	SealBend1RedoDS3006	black	fragment	0.107			
	1	3	SealBend1RedoDS3007	black	fragment	0.119			
	1	3		black	fragment	0.0889			
	1	3		black	fragment	0.0534			
	1	3	SealBend1RedoDS3008	black	fragment	0.0496			
	1	3		black	fiber	0.114			
	1	3		black	fiber	0.09			
	1	3	SealBend1RedoDS3009	black	fragment	0.0904			
	1	3		black	fragment	0.101			
	1	3	SealBend1RedoDS3010	black	fragment	0.0721			
	1	3	SealBend1RedoDS3011	black	fragment	0.0881			
	1	3		black	fragment	0.0527			
	1	3		black	fragment	0.0968			
	1	3	SealBend1RedoDS3012	black	fragment	0.0558			

	1	3		black	fragment	0.0539		
	1	3		black	fragment	0.193		
	1	3		black	fragment	0.0613	25	**50**
	2	1	SealBend2RedoDS1002	black	fragment	0.0601		
	2	1	SealBend2RedoDS1003	black	fragment	0.051		
	2	1	SealBend2RedoDS1004	black	fragment	0.172		
	2	1	SealBend2RedoDS1005	black	fragment	0.028		
	2	1	SealBend2RedoDS1006	black	fragment	0.0481		
	2	1	SealBend2RedoDS1007	black	fragment	0.0323		
	2	1		clear	fiber	0.2498		
	2	1		black	fragment	0.076		
	2	1	SealBend2RedoDS1008	black	fragment	0.0601		
	2	1	SealBend2RedoDS1009	black	fragment	0.0401		
	2	1	SealBend2RedoDS1010	black	fragment	0.0401		
	2	1	SealBend2RedoDS1011	black	fragment	0.0626		
	2	1	SealBend2RedoDS1012	black	fragment	0.0457		
	2	1		black	fragment	0.0441		
	2	1	SealBend2RedoDS1013	black	fragment	0.0401		
	2	1	SealBend2RedoDS1014	pink	Fragment	0.0481		
	2	1	SealBend2RedoDS1015	black	fragment	0.0361		
	2	1		black	fragment	0.0591		

	2	1	SealBend2RedoDS1016	black	fragment	0.0521		
	2	1	SealBend2RedoDS1017	black	fragment	0.0441		
	2	1	SealBend2RedoDS1018	black	fragment	0.0401		
	2	1	SealBend2RedoDS1020	black	fragment	0.028		
	2	1	SealBend2RedoDS1021	black	fiber	0.108	23	
	2	2	SealBend2RedoDS2001	black	fragment	0.0706		
	2	2	SealBend2RedoDS2002	black	fragment	0.113		
	2	2	SealBend2RedoDS2003	black	fragment	0.0413		
	2	2	SealBend2RedoDS2004	black	fragment	0.13		
	2	2	SealBend2RedoDS2005	black	fragment	0.0538		
	2	2	SealBend2RedoDS2006	black	fragment	0.0601		
	2	2	SealBend2RedoDS2007	black	fragment	0.0361		
	2	2		black	fragment	0.0401		
	2	2	SealBend2RedoDS2008	black	fragment	0.0513		
	2	2		black	fragment	0.0468	10	
	2	3	SealBend2RedoDS3001	black	fragment	0.0579		
	2	3	SealBend2RedoDS3002	black	fragment	0.111		
	2	3	SealBend2RedoDS3003	black	fragment	0.0479		
	2	3	SealBend2RedoDS3004	black	fragment	0.0538		
	2	3	SealBend2RedoDS3005	black	fragment	0.0483		
	2	3	SealBend2RedoDS3007	clear	fragment	0.0581		

	2	3	SealBend2RedoDS3008	black	fragment	0.0964		
	2	3	SealBend2RedoDS3009	black	fragment	0.0656		
	2	3		black	fragment	0.0914		
	2	3	SealBend2RedoDS3010	red	fiber	1.2935		
	2	3	SealBend2RedoDS3011	black	fragment	0.0751		
	2	3	SealBend2RedoDS3012	black	fragment	0.0507		
	2	3	SealBend2RedoDS3013	black	fragment	0.0707		
	2	3		black	fragment	0.0568		
	2	3	SealBend2RedoDS3014	black	fiber	0.152		
	2	3	SealBend2RedoDS3015	black	fragment	0.0313		
	2	3		black	fragment	0.051		
	2	3	SealBend2RedoDS3016	black	fragment	0.0733		
	2	3	SealBend2RedoDS3017	black	fragment	0.0409		
	2	3	SealBend2RedoDS3018	black	fragment	0.0512		
	2	3	SealBend2RedoDS3019	black	fragment	0.0734	21	**54**
Salinas River	1	1	SalinasRiver1DS1001	blue	fragment	0.112		
	1	1	SalinasRiver1DS1002	black	fragment	0.224		
	1	1	SalinasRiver1DS1003	black	fragment	0.14		
	1	1		black	fragment	0.394		
	1	1	SalinasRiver1DS1004	black	fragment	0.132		

	1	1	SalinasRiver1DS1005	black	fragment	0.184		
	1	1	SalinasRiver1DS1006	black	fragment	0.157		
	1	1	SalinasRiver1DS1007	black	fragment	0.151		
	1	1	SalinasRiver1DS1008	black	fragment	0.145		
	1	1		black	fragment	0.0596		
	1	1	SalinasRiver1DS1009	black	fragment	0.0641		
	1	1	SalinasRiver1DS1010	black	fragment	0.0574		
	1	1	SalinasRiver1DS1011	black	fragment	0.118		
	1	1	SalinasRiver1DS1012	black	fragment	0.236		
	1	1	SalinasRiver1DS1013	black	fragment	0.136		
	1	1	SalinasRiver1DS1014	black	fragment	0.209		
	1	1		black	fragment	0.116		
	1	1	SalinasRiver1DS1015	black	fragment	0.134		
	1	1		black	fragment	0.675		
	1	1		black	fragment	0.384		
	1	1		black	fragment	0.312		
	1	1		black	fragment	0.0731		
	1	1		black	fragment	0.219		
	1	1	SalinasRiver1DS1016	black	fragment	0.263		
	1	1		black	fragment	0.607		
	1	1		black	fragment	0.0717		

	1	1		black	fragment	0.112		
	1	1		black	fragment	0.157		
	1	1		black	fragment	0.337		
	1	1	SalinasRiver1DS1017	black	fragment	0.127		
	1	1	SalinasRiver1DS1018	black	fragment	0.0985		
	1	1	SalinasRiver1DS1019	black	fragment	0.0875		
	1	1	SalinasRiver1DS1020	black	fiber	0.6408		
	1	1	SalinasRiver1DS1021	black	fragment	0.0881		
	1	1	SalinasRiver1DS1022	black	fragment	0.0801	35	
	1	2	SalinasRiver1DS2001	blue	fragment	0.224		
	1	2	SalinasRiver1DS2002	black	fragment	0.0721		
	1	2	SalinasRiver1DS2003	black	fragment	0.0561		
	1	2	SalinasRiver1DS2004	black	fragment	0.0881		
	1	2	SalinasRiver1DS2005	black	fragment	0.386		
	1	2		black	fragment	0.103		
	1	2		black	fragment	0.128		
	1	2		black	fragment	0.107		
	1	2	SalinasRiver1DS2006	black	fragment	0.343		
	1	2	SalinasRiver1DS2007	black	fiber	0.2212		
	1	2	SalinasRiver1DS2008	black	fragment	0.0489		
	1	2	SalinasRiver1DS2009	black	fragment	0.137		

	1	2	SalinasRiver1DS2010	black	fragment	0.141		
	1	2		black	fragment	0.0921		
	1	2	SalinasRiver1DS2011	black	fragment	0.0795		
	1	2	SalinasRiver1DS2012	black	fragment	0.0801	16	
	1	3	SalinasRiver1DS3001	black	fragment	0.205		
	1	3	SalinasRiver1DS3002	black	fragment	0.148		
	1	3	SalinasRiver1DS3003	black	fragment	0.0444		
	1	3	SalinasRiver1DS3004	black	fragment	0.0589		
	1	3	SalinasRiver1DS3005	black	fragment	0.0514		
	1	3	SalinasRiver1DS3006	black	fragment	0.212		
	1	3	SalinasRiver1DS3007	black	fragment	0.0551		
	1	3	SalinasRiver1DS3008	black	fragment	0.347		
	1	3		black	fiber	0.263		
	1	3		black	fragment	0.156		
	1	3	SalinasRiver1DS3009	black	fragment	0.186		
	1	3	SalinasRiver1DS3010	black	fragment	0.0739		
	1	3	SalinasRiver1DS3011	black	fragment	0.0428		
	1	3	SalinasRiver1DS3012	black	fragment	0.266		
	1	3	SalinasRiver1DS3013	black	fragment	0.0493		
	1	3	SalinasRiver1DS3014	black	fragment	0.0456		
	1	3	SalinasRiver1DS3015	black	fragment	0.0527		

	1	3	SalinasRiver1DS3016	black	fragment	0.0451		
	1	3		black	fragment	0.0577		
	1	3	SalinasRiver1DS3017	black	fragment	0.0865		
	1	3	SalinasRiver1DS3018	black	fragment	0.0426		
	1	3	SalinasRiver1DS3019	black	fragment	0.137		
	1	3	SalinasRiver1DS3020	black	fragment	0.244		
	1	3	SalinasRiver1DS3021	green	fiber	2.0837		
	1	3	SalinasRiver1DS3022	blue	fiber	0.9656		
	1	3	SalinasRiver1DS3023	black	fiber	0.3369		
	1	3	SalinasRiver1DS3024	black	fragment	0.0932		
	1	3	SalinasRiver1DS3025	black	fragment	0.0844		
	1	3	SalinasRiver1DS3026	black	fragment	0.162		
	1	3		black	fragment	0.132		
	1	3	SalinasRiver1DS3027	black	fiber	0.513	31	82
	2	1	SalinasRiver2DS1001	black	fragment	0.0634		
	2	1	SalinasRiver2DS1002	black	fragment	0.0594		
	2	1	SalinasRiver2DS1003	black	fragment	0.0724		
	2	1	SalinasRiver2DS1004	black	fragment	0.11		
	2	1		blue	fragment	0.0511		
	2	1	SalinasRiver2DS1005	black	fragment	0.0655		
	2	1	SalinasRiver2DS1006	black	fragment	0.0517		

	2	1	SalinasRiver2DS1007	blue	fragment	0.157		
	2	1	SalinasRiver2DS1008	black	fragment	0.0764		
	2	1	SalinasRiver2DS1009	black	fragment	0.153		
	2	1	SalinasRiver2DS1010	blue	fragment	0.801		
	2	1	SalinasRiver2DS1011	black	fragment	0.101		
	2	1		black	fragment	0.105		
	2	1	SalinasRiver2DS1012	black	fiber	0.291		
	2	1		black	fragment	0.11		
	2	1	SalinasRiver2DS1013	black	fragment	0.0638		
	2	1	SalinasRiver2DS1014	black	fragment	0.143		
	2	1	SalinasRiver2DS1015	black	fragment	0.0733		
	2	1	SalinasRiver2DS1016	black	fragment	0.0623		
	2	1	SalinasRiver2DS1017	black	fragment	0.103		
	2	1	SalinasRiver2DS1018	black	fragment	0.107		
	2	1	SalinasRiver2DS1019	black	fragment	0.0974		
	2	1	SalinasRiver2DS1020	black	fiber	0.164		
	2	1	SalinasRiver2DS1021	black	fragment	0.125		
	2	1	SalinasRiver2DS1022	black	fragment	0.132		
	2	1	SalinasRiver2DS1023	black	fiber	0.0932	26	
	2	2	SalinasRiver2DS2001	black	fragment	0.0457		
	2	2		black	fragment	0.07		

	2	2	SalinasRiver2DS2002	black	fragment	0.0601		
	2	2	SalinasRiver2DS2003	black	fragment	0.0583		
	2	2	SalinasRiver2DS2004	black	fragment	0.133		
	2	2	SalinasRiver2DS2005	black	fragment	0.155		
	2	2	SalinasRiver2DS2006	black	fragment	0.118		
	2	2	SalinasRiver2DS2007	black	fiber	1.6865		
	2	2	SalinasRiver2DS2008	black	fragment	0.0778		
	2	2	SalinasRiver2DS2009	black	fragment	0.125		
	2	2	SalinasRiver2DS2010	blue	fragment	0.0713		
	2	2	SalinasRiver2DS2011	black	fragment	0.407		
	2	2	SalinasRiver2DS2012	black	fragment	0.0401	13	
	2	3	SalinasRiver2DS3001	black	fragment	0.197		
	2	3	SalinasRiver2DS3002	blue	fragment	0.485		
	2	3	SalinasRiver2DS3003	black	fragment	0.14		
	2	3	SalinasRiver2DS3004	black	fragment	0.109		
	2	3	SalinasRiver2DS3005	black	fragment	0.071		
	2	3	SalinasRiver2DS3006	black	fragment	0.0896		
	2	3	SalinasRiver2DS3007	black	fragment	0.0457		
	2	3	SalinasRiver2DS3008	black	fragment	0.028		
	2	3		black	fragment	0.0363		
	2	3	SalinasRiver2DS3009	black	fragment	0.2325		

	2	3	SalinasRiver2DS3010	black	fragment	0.127		
	2	3	SalinasRiver2DS3011	black	fragment	0.108		
	2	3	SalinasRiver2DS3012	black	fragment	0.0938		
	2	3	SalinasRiver2DS3013	black	fragment	0.0685		
	2	3	SalinasRiver2DS3014	black	fragment	0.214		
	2	3	SalinasRiver2DS3015	black	fragment	0.068	16	**42**
	3	1	SalinasRiver3DS1001	black	fragment	0.196		
	3	1	SalinasRiver3DS1002	black	fragment	0.0761		
	3	1	SalinasRiver3DS1003	black	fragment	0.0481		
	3	1	SalinasRiver3DS1004	black	fragment	0.1		
	3	1	SalinasRiver3DS1005	black	fragment	0.0507		
	3	1		black	fragment	0.0681		
	3	1	SalinasRiver3DS1006	black	fragment	0.0442		
	3	1	SalinasRiver3DS1007	black	fiber	0.119		
	3	1		black	fiber	0.0596		
	3	1	SalinasRiver3DS1008	black	fragment	0.0521		
	3	1	SalinasRiver3DS1009	black	fragment	0.0978		
	3	1	SalinasRiver3DS1010	black	fragment	0.0633		
	3	1		black	fragment	0.0992		
	3	1	SalinasRiver3DS1011	black	fiber	0.12		
	3	1	SalinasRiver3DS1012	black	fiber	0.0882		

	3	1	SalinasRiver3DS1013	black	fragment	0.0935		
	3	1		black	fragment	0.0401		
	3	1	SalinasRiver3DS1014	black	fragment	0.0771		
	3	1	SalinasRiver3DS1015	black	fragment	0.0522	19	
	3	2	SalinasRiver3DS2001	black	fragment	0.0677		
	3	2	SalinasRiver3DS2002	blue	fiber	0.8074		
	3	2	SalinasRiver3DS2003	black	fragment	0.0885		
	3	2	SalinasRiver3DS2004	black	fragment	0.0793		
	3	2	SalinasRiver3DS2005	black	fragment	0.0606		
	3	2	SalinasRiver3DS2006	black	fragment	0.0313		
	3	2		black	fragment	0.03		
	3	2	SalinasRiver3DS2007	black	fragment	0.151		
	3	2	SalinasRiver3DS2008	black	fragment	0.0626		
	3	2	SalinasRiver3DS2009	black	fragment	0.194		
	3	2	SalinasRiver3DS2010	black	fragment	0.13		
	3	2	SalinasRiver3DS2011	blue	fragment	0.082	12	
	3	3	SalinasRiver3DS3001	black	fragment	0.162		
	3	3	SalinasRiver3DS3002	black	fragment	0.0439		
	3	3		black	fragment	0.0739		
	3	3		black	fragment	0.0714		
	3	3	SalinasRiver3DS3003	black	fragment	0.0951		

	3	3	SalinasRiver3DS3004	black	fragment	0.124		
	3	3	SalinasRiver3DS3005	black	fragment	0.0714		
	3	3	SalinasRiver3DS3006	black	fragment	0.0747		
	3	3		black	fragment	0.0913		
	3	3	SalinasRiver3DS3007	black	fragment	0.159		
	3	3		black	fragment	0.271		
	3	3	SalinasRiver3DS3008	black	fragment	0.0643		
	3	3	SalinasRiver3DS3009	black	fragment	0.0941		
	3	3		black	fragment	0.0745		
	3	3	SalinasRiver3DS3010	black	fragment	0.147		
	3	3	SalinasRiver3DS3011	black	fragment	0.122		
	3	3		black	fragment	0.0646		
	3	3	SalinasRiver3DS3012	black	fragment	0.0931		
	3	3		black	fragment	0.11		
	3	3	SalinasRiver3DS3013	black	fragment	0.0551		
	3	3		black	fragment	0.0588		
	3	3	SalinasRiver3DS3014	black	fragment	0.0853		
	3	3	SalinasRiver3DS3015	black	fragment	0.0577		
	3	3		black	fragment	0.0724		
	3	3	SalinasRiver3DS3016	black	Fragment	0.0923		
	3	3	SalinasRiver3DS3017	black	fragment	0.0469		

	3	3	SalinasRiver3DS3018	black	fragment	0.101		
	3	3		black	fragment	0.0521		
	3	3		black	fragment	0.207		
	3	3	SalinasRiver3DS3019	black	fragment	0.0577		
	3	3	SalinasRiver3DS3020	black	fragment	0.0933		
	3	3	SalinasRiver3DS3021	black	fragment	0.051		
	3	3	SalinasRiver3DS3022	black	fragment	0.0463		
	3	3		black	fragment	0.0351		
	3	3	SalinasRiver3DS3023	blue	fragment	0.0372		
	3	3	SalinasRiver3DS3024	black	fragment	0.384		
	3	3	SalinasRiver3DS3025	black	fragment	0.149		
	3	3	SalinasRiver3DS3026	black	fragment	0.0659		
	3	3	SalinasRiver3DS3027	black	fragment	0.0521		
	3	3	SalinasRiver3DS3028	black	fragment	0.0587		
	3	3	SalinasRiver3DS3029	black	fragment	0.0539		
	3	3		black	fragment	0.377		
	3	3	SalinasRiver3DS3030	black	fiber	1.4013		
	3	3	SalinasRiver3DS3031	blue	fragment	0.163	44	**75**
	4	1	SalinasRiver4DS1001	black	fiber	1.5618		
	4	1	SalinasRiver4DS1002	black	fiber	0.2822		
	4	1	SalinasRiver4DS1003	black	fragment	0.0903		

	4	1	SalinasRiver4DS1004	black	fragment	0.14		
	4	1	SalinasRiver4DS1005	black	fragment	0.173		
	4	1	SalinasRiver4DS1006	black	fragment	0.124		
	4	1	SalinasRiver4DS1007	black	fragment	0.24		
	4	1		black	fragment	0.118		
	4	1	SalinasRiver4DS1008	black	fragment	0.0592		
	4	1	SalinasRiver4DS1009	black	fragment	0.128		
	4	1	SalinasRiver4DS1010	black	fragment	0.155		
	4	1	SalinasRiver4DS1011	black	fragment	0.118		
	4	1	SalinasRiver4DS1012	blue	fragment	0.0569	13	
	4	2	SalinasRiver4DS2001	black	fragment	0.0854		
	4	2	SalinasRiver4DS2002	black	fragment	0.174		
	4	2	SalinasRiver4DS2003	black	fragment	0.0838		
	4	2	SalinasRiver4DS2004	black	fragment	0.145		
	4	2	SalinasRiver4DS2005	black	fragment	0.0425		
	4	2		black	fragment	0.0277		
	4	2	SalinasRiver4DS2006	black	fragment	0.0372		
	4	2	SalinasRiver4DS2007	blue	fragment	0.0615		
	4	2	SalinasRiver4DS2008	black	fragment	0.0621		
	4	2		black	fragment	0.004		
	4	2	SalinasRiver4DS2009	green	fragment	0.0632		

	4	2	SalinasRiver4DS2010	green	fragment	0.0644		
	4	2	SalinasRiver4DS2011	black	fragment	0.0477		
	4	2	SalinasRiver4DS2012	black	fragment	0.101		
	4	2	SalinasRiver4DS2013	black	fragment	0.231		
	4	2	SalinasRiver4DS2014	blue	fragment	0.154		
	4	2	SalinasRiver4DS2015	black	fragment	0.0383		
	4	2	SalinasRiver4DS2016	black	fragment	0.0577		
	4	2	SalinasRiver4DS2017	black	fragment	0.127	19	
	4	3	SalinasRiver4DS3001	black	fragment	0.0276		
	4	3		clear	fragment	0.162		
	4	3	SalinasRiver4DS3002	black	fragment	0.0411		
	4	3		black	fragment	0.0409		
	4	3	SalinasRiver4DS3003	black	fragment	0.0511		
	4	3		black	fragment	0.0754		
	4	3	SalinasRiver4DS3004	black	fragment	0.0556		
	4	3		black	fragment	0.114		
	4	3	SalinasRiver4DS3005	black	fragment	0.0636		
	4	3	SalinasRiver4DS3006	black	fragment	0.132		
	4	3	SalinasRiver4DS3007	black	fragment	0.0747		
	4	3	SalinasRiver4DS3008	black	fragment	0.0519		
	4	3	SalinasRiver4DS3009	black	fragment	0.124		

	4	3	SalinasRiver4DS3010	black	fragment	0.146		
	4	3	SalinasRiver4DS3011	black	fragment	0.0531		
	4	3	SalinasRiver4DS3012	black	fragment	0.0486		
	4	3	SalinasRiver4DS3013	black	fiber	0.131		
	4	3	SalinasRiver4DS3014	black	fiber	0.109		
	4	3	SalinasRiver4DS3015	black	fragment	0.0799		
	4	3	SalinasRiver4DS3016	black	fragment	0.089		
	4	3	SalinasRiver4DS3017	black	fragment	0.0589		
	4	3	SalinasRiver4DS3018	black	fragment	0.2195		
	4	3	SalinasRiver4DS3019	black	fragment	0.0696		
	4	3	SalinasRiver4DS3020	black	fragment	0.0393		
	4	3	SalinasRiver4DS3021	black	fragment	0.232		
	4	3	SalinasRiver4DS3022	black	fragment	0.111		
	4	3	SalinasRiver4DS3023	black	fragment	0.0705	27	**40**
Parsons	1	1	Parsons1RedoDS1001	black	fiber	0.584		
	1	1	Parsons1RedoDS1002	black	fiber	0.123		
	1	1	Parsons1RedoDS1003	black	fiber	0.288	3	
	1	2	Parsons1RedoDS2001	black	fragment	0.0713		
	1	2	Parsons1RedoDS2002	black	fragment	0.0867		
	1	2	Parsons1RedoDS2003	black	fiber	0.0596	3	
	1	3	Parsons1RedoDS3001	blue	fragment	0.124		

	1	3	Parsons1RedoDS3002	blue	fragment	0.0881		
	1	3	Parsons1RedoDS3003	blue	fiber	0.4116	3	**9**
	2	1	Parsons2RedoDS1001	blue	fragment	0.0606		
	2	1	Parsons2RedoDS1002	blue	fragment	0.0778		
	2	1	Parsons2RedoDS1003	black	fragment	0.0433		
	2	1	Parsons2RedoDS1004	black	fragment	0.0882		
	2	1	Parsons2RedoDS1005	black	fragment	0.0641		
	2	1	Parsons2RedoDS1006	black	fragment	0.0596		
	2	1	Parsons2RedoDS1007	black	fragment	0.0513		
	2	1	Parsons2RedoDS1008	black	fragment	0.0401		
	2	1	Parsons2RedoDS1009	black	fragment	0.1		
	2	1	Parsons2RedoDS1010	black	fiber	0.0787	10	
	2	2	Parsons2RedoDS2001	black	fragment	0.33		
	2	2	Parsons2RedoDS2002	black	fiber	0.131		
	2	2	Parsons2RedoDS2003	blue	fragment	0.0441		
	2	2	Parsons2RedoDS2004	black	fragment	0.0426		
	2	2	Parsons2RedoDS2005	black	fragment	0.0811		
	2	2	Parsons2RedoDS2006	black	fragment	0.324		
	2	2	Parsons2RedoDS2007	black	fragment	0.121		
	2	2	Parsons2RedoDS2008	black	fragment	0.0739		
	2	2	Parsons2RedoDS2009	black	fiber	0.105		

	2	2	Parsons2RedoDS2010	black	fragment	0.0908		
	2	2	Parsons2RedoDS2011	black	fragment	0.0403		
	2	2	Parsons2RedoDS2012	black	fragment	0.0686		
	2	2	Parsons2RedoDS2013	black	fragment	0.0431		
	2	2		blue	fragment	0.192		
	2	2	Parsons2RedoDS2014	black	fragment	0.0682		
	2	2	Parsons2RedoDS2015	black	fragment	0.0626		
	2	2	Parsons2RedoDS2016	black	fragment	0.0762		
	2	2	Parsons2RedoDS2017	black	fragment	0.0457		
	2	2	Parsons2RedoDS2018	black	fragment	0.108		
	2	2	Parsons2RedoDS2019	black	fragment	0.09	20	
	2	3	Parsons2RedoDS3001	black	fragment	0.139		
	2	3	Parsons2RedoDS3002	black	fragment	0.0521		
	2	3	Parsons2RedoDS3003	black	fragment	0.0441		
	2	3	Parsons2RedoDS3004	black	fragment	0.0774		
	2	3	Parsons2RedoDS3005	black	fragment	0.0481		
	2	3		black	fragment	0.0521		
	2	3	Parsons2RedoDS3006	black	fragment	0.0481		
	2	3	Parsons2RedoDS3007	black	fragment	0.0426		
	2	3	Parsons2RedoDS3008	black	fragment	0.051		
	2	3	Parsons2RedoDS3009	black	fragment	0.0633		

	2	3	Parsons2RedoDS3010	black	fragment	0.0627		
	2	3	Parsons2RedoDS3011	black	fragment	0.0611		
	2	3	Parsons2RedoDS3012	black	fragment	0.0602		
	2	3	Parsons2RedoDS3013	black	fragment	0.0921		
	2	3	Parsons2RedoDS3014	black	fragment	0.0761		
	2	3	Parsons2RedoDS3015	pink	Fragment	0.0647		
	2	3	Parsons2RedoDS3016	black	fiber	0.774		
	2	3	Parsons2RedoDS3017	black	fragment	0.0567	18	**48**
	3	1	Parsons3RedoDS1001	blue	fragment	0.061		
	3	1	Parsons3RedoDS1002	black	fragment	0.0522		
	3	1	Parsons3RedoDS1003	black	fragment	0.0561		
	3	1	Parsons3RedoDS1004	black	fragment	0.0361	4	
	3	2	Parsons3RedoDS2001	black	fragment	0.0521		
	3	2	Parsons3RedoDS2002	black	fragment	0.0641		
	3	2	Parsons3RedoDS2003	blue	fragment	0.0426		
	3	2	Parsons3RedoDS2004	black	fragment	0.0753	4	
	3	3	Parsons3RedoDS3001	black	fiber	0.6915		
	3	3	Parsons3RedoDS3002	black	fragment	0.0441		
	3	3	Parsons3RedoDS3003	black	fragment	0.0521	3	**11**
	4	1	Parsons4RedoDS1001	black	fragment	0.0441		
	4	1	Parsons4RedoDS1002	black	fragment	0.0401		

	4	1	Parsons4RedoDS1003	black	fragment	0.032		
	4	1	Parsons4RedoDS1004	black	fragment	0.0601		
	4	1	Parsons4RedoDS1005	black	fragment	0.121	5	
	4	2	Parsons4RedoDS2001	black	fragment	0.0361		
	4	2	Parsons4RedoDS2002	black	fiber	0.9546		
	4	2	Parsons4RedoDS2003	black	fragment	0.0412		
	4	2	Parsons4RedoDS2004	black	fiber	0.086	4	
	4	3	Parsons4RedoDS3001	black	fragment	0.0602		
	4	3	Parsons4RedoDS3002	black	fragment	0.032		
	4	3	Parsons4RedoDS3003	blue	fragment	0.0561		
	4	3	Parsons4RedoDS3004	black	fragment	0.0513		
	4	3		black	fragment	0.0481		
	4	3	Parsons4RedoDS3005	black	fragment	0.0539		
	4	3	Parsons4RedoDS3006	black	fragment	0.0484		
	4	3	Parsons4RedoDS3007	black	fragment	0.0361		
	4	3	Parsons4RedoDS3008	black	fragment	0.0441		
	4	3	Parsons4RedoDS3009	black	fragment	0.0481		
	4	3	Parsons4RedoDS3010	black	fragment	0.0481	11	**20**
Total MPs 1024			Total Fragments 916			Total Fibers 108		
Mean Length (mm) .134			SD (mm) .245	Median (mm) 0.066		Mode (mm) 0.0481		

APPENDIX B

SAMPLE MASSES AND DENSITIES OF NACL SOLUTION USED FOR DENSITY SEPARATIONS

Sample Name	Sample Mass (g)	DS 1 Density (g/cm^3)	DS 2 Density (g/cm^3)	DS 3 Density (g/cm^3)	Average Density (g/cm^3)	Total Sediment Mass of Sample Area (g)	Total MPs in Sample Area	Concentration (items/kg wet sediment)
Azevedo Ag 1	50	1.21	1.225	1.21	1.215			
Azevedo Ag 2	50	1.22	1.215	1.215	1.216667			
Azevedo Ag 3	52	1.19	1.185	1.19	1.188333			
Ag Site 1	51	1.18	1.195	1.205	1.193333	203	116	571.4286
Azevedo1	47	1.205	1.235	1.205	1.215			
Azevedo2	51	1.175	1.185	1.185	1.181667			
Azevedo3	26	1.18	1.19	1.19	1.186667			
Azevedo4	50	1.18	1.2	1.195	1.191667	174	97	557.4713
Bird 1	51	1.19	1.215	1.215	1.206667			
Bird 2	52	1.185	1.195	1.195	1.191667			
Bird 3	52	1.192	1.185	1.185	1.187333			
Bird 4	52	1.185	1.185	1.185	1.185	207	206	995.1691
Hester 1	50	1.175	1.185	1.185	1.181667			
Hester 2	51	1.19	1.185	1.19	1.188333			
Hester 3	51	1.19	1.225	1.185	1.2			
Hester 4	51	1.19	1.19	1.215	1.198333	203	142	699.5074

Seal Bend 1	50	1.19	1.2	1.21	1.2			
Seal Bend 2	51	1.19	1.185	1.185	1.186667	101	104	1029.703
Salinas River 1	50	1.205	1.21	1.17	1.195			
Salinas River 2	52	1.21	1.205	1.22	1.211667			
Salinas River 3	50	1.205	1.215	1.17	1.196667			
Salinas River 4	51	1.195	1.205	1.215	1.205	203	271	1334.975
Parsons 1	47	1.18	1.225	1.21	1.205			
Parsons 2	51	1.195	1.215	1.215	1.208333			
Parsons 3	50	1.2	1.22	1.205	1.208333			
Parsons 4	49	1.215	1.2	1.175	1.196667	197	88	446.7005
								804.9936
				Average density for all density seps	1.197718		Note: Seal Bend 3 & 4 excluded	

APPENDIX C

Student T Test Results

P value < .05 indicated by “1”   P value >.05 indicated by “0”

Test for all MPs lengths							
Agriculture	0	1	1	1	1	1	1
Azevedo	1	0	0	0	0	0	0
Bird	1	0	0	0	0	1	0
Hester	1	0	0	0	0	1	0
Seal Bend	1	0	0	0	0	1	0
Old Salinas River	1	0	1	1	1	0	0
Parsons	1	0	0	0	0	0	0
	Agriculture	**Azevedo**	**Bird**	**Hester**	**Seal Bend**	**Old Salinas River**	**Parsons**

Test for fragment lengths only							
Agriculture	0	0	1	1	1	0	1
Azevedo	0	0	1	1	0	0	0
Bird	1	1	0	0	0	1	0
Hester	1	1	0	0	0	1	0
Seal Bend	1	0	0	0	0	1	0
Old Salinas River	0	0	1	1	1	0	1
Parsons	1	0	0	0	0	1	0
	Agriculture	**Azevedo**	**Bird**	**Hester**	**Seal Bend**	**Old Salinas River**	**Parsons**
Test for fiber lengths only							
Agriculture	0	1	1	1	1	1	1
Azevedo	1	0	0	0	0	0	0
Bird	1	0	0	0	0	0	0
Hester	1	0	0	0	0	0	0
Seal Bend	1	0	0	0	0	0	0
Old Salinas River	1	0	0	0	0	0	0
Parsons	1	0	0	0	0	0	0

	Agriculture	Azevedo	Bird	Hester	Seal Bend	Old Salinas River	Parsons

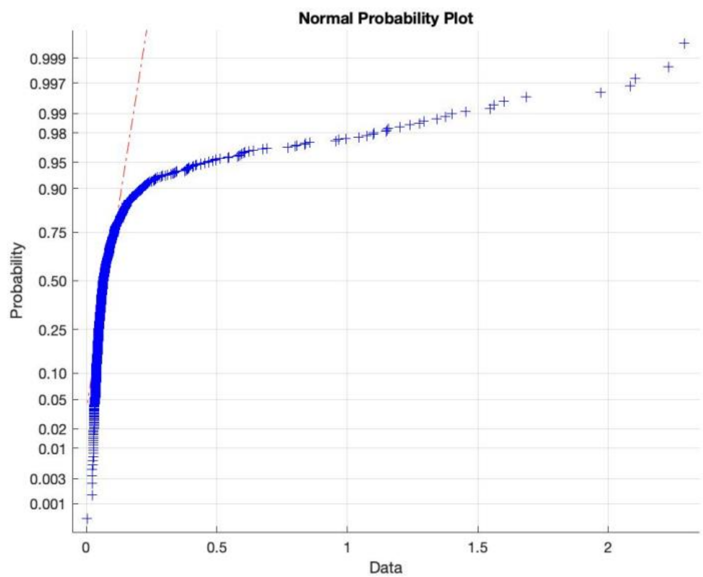

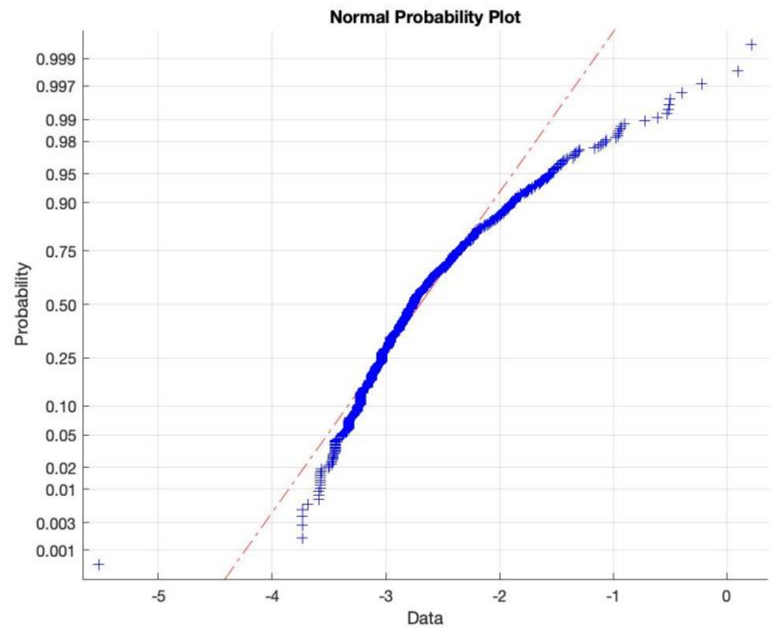

Log Transformed

Appendix D

Sample collecting and processing flow chart

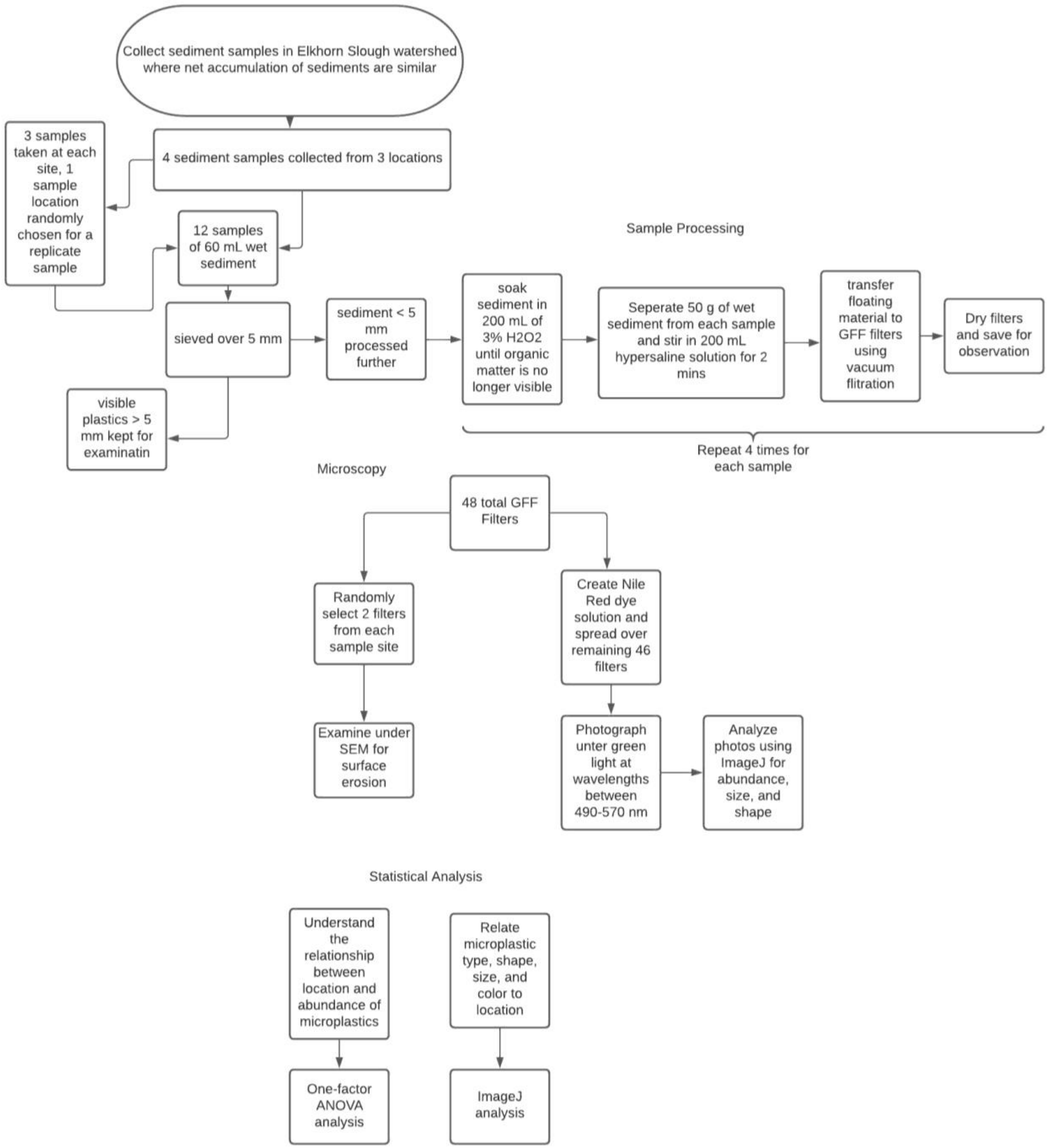

Collect sediment samples in Elkhorn Slough watershed where net accumulation of sediments are similar
4 sediment samples collected from 3 locations
3 samples taken at each site, 1 sample location randomly chosen for a replicate sample
12 samples of 60 mL wet sediment
sieved over 5 mm
visible plastics > 5 mm kept for examinatin
sediment < 5 mm processed further
Sample Processing
soak sediment in 200 mL of 3% H2O2 until organic matter is no longer visible
Seperate 50 g of wet sediment from each sample and stir in 200 mL hypersaline solution for 2 mins
transfer floating material to GFF filters using vacuum flitration
Dry filters and save for observation
Repeat 4 times for each sample
Microscopy
48 total GFF Filters
Randomly select 2 filters from each sample site
Examine under SEM for surface erosion
Create Nile Red dye solution and spread over remaining 46 filters
Photograph unter green light at wavelengths between 490-570 nm
Analyze photos using ImageJ for abundance, size, and shape
Statistical Analysis
Understand the relationship between location and abundance of microplastics
One-factor ANOVA analysis
Relate microplastic type, shape, size, and color to location
ImageJ analysis

Appendix E

Grain size statistics on soil samples

LS	File name:	File ID:	From	To	Volume	Mean:	Median:	Mode:	S.D.:	Skewness:	Kurtosis:	% <	10	25	50	75	90	Volume % <	4	6	10	32	63	125	250	500	% Clay	%Silt	%Sand
#########	Azevedo1_3866.$ls	Azevedo1	0.03999	2000	100	3.38306	3.70059	12.3958	2.73652	-0.44411	-0.58561	Size	13.6864	81.6323	100	100	0		52.8699	66.8743	81.6325	100	100	100	100	100	52.8699	47.1301	0
#########	Azevedo2_3867.$ls	Azevedo2	0.03999	2000	100	12.9988	15.0343	14.938	3.21625	-0.72209	0.196368	Size	3.62855	34.9007	99.9981	100	0		15.4641	23.2875	34.9008	75.3813	93.6834	100	100	100	15.4641	78.2193	6.3166
#########	Azevedo3_3868.$ls	Azevedo3	0.03999	2000	100	3.29412	3.62575	12.3958	2.78609	-0.42474	-0.65051	Size	14.7927	81.8338	100	100	0		53.4896	67.1581	81.834	100	100	100	100	100	53.4896	46.5104	0
#########	Azevedo4_3869.$ls	Azevedo4	0.03999	2000	100	3.16129	3.40583	12.3958	2.75179	-0.36897	-0.65204	Size	15.001	83.3366	100	100	0		55.8579	69.5487	83.3367	100	100	100	100	100	55.8579	44.1421	0
#########	Bird1_3858.$ls	Bird1	0.03999	2000	100	4.1102	4.34347	4.04727	2.70848	-0.46056	-0.21865	Size	9.21153	77.9593	100	100	0		46.669	62.5574	77.9594	100	100	100	100	100	46.669	53.331	0
#########	Bird2_3859.$ls	Bird2	0.03999	2000	100	5.05268	5.61823	18.0016	3.32399	-0.47553	-0.60844	Size	11.0645	63.2841	100	100	0		40.9756	51.6101	63.2842	98.7823	100	100	100	100	40.9756	59.0244	0
#########	Bird3_3860.$ls	Bird3	0.03999	2000	100	5.41381	6.0107	18.0016	3.41406	-0.46316	-0.58558	Size	10.4723	61.184	100	100	0		39.502	49.9558	61.1841	96.326	100	100	100	100	39.502	60.498	0
#########	Bird4_3861.$ls	Bird4	0.03999	2000	100	5.53895	6.40376	16.3984	3.19552	-0.59612	-0.2553	Size	9.14066	61.8535	100	100	0		36.7588	48.2218	61.8536	97.4775	100	100	100	100	36.7588	63.2412	0
#########	Hester1_3845.$ls	Hester1	0.03999	2000	100	14.4856	16.3644	14.938	3.07757	-0.77482	0.519737	Size	2.9083	30.8563	99.7347	100	0		12.6794	19.7085	30.8565	73.7984	93.3765	100	100	100	12.6794	80.6971	6.6235
#########	Hester2_2_3847.$ls	Hester2_2	0.03999	2000	100	14.6088	16.6423	14.938	3.39163	-0.73053	0.123333	Size	3.479	32.7869	99.8997	100	0		14.7805	22.3387	32.787	68.757	90.6795	100	100	100	14.7805	75.899	9.3205
#########	Hester3_3848.$ls	Hester3	0.03999	2000	100	2.55492	2.73341	3.68682	2.57543	-0.239	-0.6821	Size	18.3473	92.0144	100	100	0		64.7651	79.6443	92.0145	100	100	100	100	100	64.7651	35.2349	0
#########	Hester4_3849.$ls	Hester4	0.03999	2000	100	10.2416	12.5049	14.938	2.96585	-0.76214	0.232616	Size	4.04718	41.2662	100	100	0		18.4312	27.8262	41.2663	85.4692	99.9274	100	100	100	18.4312	81.4962	0.0726
#########	Parsons1_3854.$ls	Parsons1	0.03999	2000	100	6.24871	7.40969	18.0016	3.433	-0.50234	-0.67024	Size	9.42785	56.1786	100	100	0		35.5211	45.3421	56.1787	94.2107	100	100	100	100	35.5211	64.4789	0
#########	Parsons2_3855.$ls	Parsons2	0.03999	2000	100	10.6649	12.9027	13.6076	3.14014	-0.68995	-0.02877	Size	4.14928	40.9436	100	100	0		19.1804	28.4296	40.9437	81.1397	99.6602	100	100	100	19.1804	80.4798	0.3398
#########	Parsons3_3856.$ls	Parsons3	0.03999	2000	100	7.08927	9.55572	18.0016	3.4241	-0.64078	-0.51922	Size	8.5053	51.0004	100	100	0		31.5278	40.4475	51.0005	93.3651	100	100	100	100	31.5278	68.4722	0
#########	Parsons4_3857.$ls	Parsons4	0.03999	2000	100	9.44931	12.6047	41.6768	3.69782	-0.64301	-0.5291	Size	6.803	44.4635	100	100	0		26.6784	34.4227	44.4635	77.0276	99.9953	100	100	100	26.6784	73.3169	0.0047
#########	SalinasRiv_3862.$ls	SalinasRiver	0.03999	2000	100	2.57425	2.83471	4.04727	2.70665	-0.33676	-0.62147	Size	19.2194	90.9335	100	100	0		62.8756	77.8503	90.9335	100	100	100	100	100	62.8756	37.1244	0
#########	SalinasRiv_3863.$ls	SalinasRiver	0.03999	2000	100	2.98938	3.23842	4.04727	2.70789	-0.33756	-0.63744	Size	15.813	86.1874	100	100	0		57.9786	72.5711	86.1875	100	100	100	100	100	57.9786	42.0214	0
#########	SalinasRiv_3864.$ls	SalinasRiver	0.03999	2000	100	3.05895	3.48341	12.3958	3.13425	-0.61409	-0.22819	Size	17.3935	80.5927	100	100	0		54.6588	67.2702	80.5929	100	100	100	100	100	54.6588	45.3412	0
#########	SalinasRiv_3865.$ls	SalinasRiver	0.03999	2000	100	2.96218	3.23542	4.04727	2.71058	-0.36018	-0.5905	Size	15.9855	86.6931	100	100	0		58.1733	73.1111	86.6932	100	100	100	100	100	58.1733	41.8267	0
#########	SealBend1_3850.$ls	SealBend1	0.03999	2000	100	3.05621	3.23505	3.68682	2.73055	-0.28916	-0.58469	Size	15.0347	85.3353	100	100	0		58.0811	72.4691	85.3354	100	100	100	100	100	58.0811	41.9189	0
#########	SealBend2_3851.$ls	SealBend2	0.03999	2000	100	2.9865	3.1836	12.3958	2.72289	-0.33229	-0.59956	Size	15.5864	85.4426	100	100	0		58.6118	72.5714	85.4427	100	100	100	100	100	58.6118	41.3882	0
#########	SealBend3_3852.$ls	SealBend3	0.03999	2000	100	3.50602	3.71063	14.938	2.78943	-0.32887	-0.58411	Size	12.8621	80.7328	100	100	0		52.7994	67.2454	80.7329	100	100	100	100	100	52.7994	47.2006	0
#########	SealBend4_3853.$ls	SealBend4	0.03999	2000	100	2.88803	3.08046	3.68682	2.70999	-0.30166	-0.63529	Size	16.3216	86.7179	100	100	0		59.805	73.8406	86.718	100	100	100	100	100	59.805	40.195	0
#########	Agricultur_4044.$ls	Agriculture	0.03999	2000	100	24.7709	37.9844	50.2244	4.26384	-1.22825	1.10436	Size	4.3274	21.3679	86.8734	100	0		13.1	16.3558	21.3679	44.2785	71.1261	94.648	100	100	13.1	58.0261	28.8739
#########	Agricultur_4045.$ls	Agriculture	0.03999	2000	100	4.27961	4.38498	18.0014	3.02014	-0.38492	-0.60286	Size	10.787	70.8705	100	100	0		47.0004	59.4223	70.8705	100	100	100	100	100	47.0004	52.9996	0
#########	Agricultur_4046.$ls	Agriculture	0.03999	2000	100	4.2452	4.23946	18.0014	2.89685	-0.32354	-0.59995	Size	9.73606	72.6362	100	100	0		47.8921	61.1814	72.6362	100	100	100	100	100	47.8921	52.1079	0
#########	Agricultur_4047.$ls	Agriculture	0.03999	2000	100	5.66702	6.03948	18.0014	3.48731	-0.51371	-0.30591	Size	9.2745	60.4319	100	100	0		38.9921	49.8363	60.4319	94.7099	100	100	100	100	38.9921	61.0079	0

Appendix F

Full concentration comparison table

Location	Habitat Type	Sediment/Energy level	Sampling Locations	Average (mean) Abundance of microplastics/ kg	MP types found	Most abundant type of MP found	size ranges	most abundant size range	potential sources	Citation
Belgium Beach	2 depositional & 1 erosional beaches	sand	intertidal	92.8	fibers, granules, plastic films, PS spheres	fibers (59%)	N/A	N/A	harbors, plastic industries	Claessens et al., 2011
Tributaries of the River Thames basin, UK	River	N/A	intertidal	350	fibers, fragments, films	Fragments (49.3%) fibers (47.4%)	N/A	N/A	Stormwater, roadmarking paints	Horton et al., 2016
Main River, Germany	River	N/A	intertidal	1077	fibers, fragments, spheres, pellets	Fragments (51% for 630–5000 µm)	.063–.2 mm, .2–.63 mm, .63–5 mm	.2–.63 mm	Sewage treatment plants, plastic processing industry,	Klein et al., 2015
Rhine River Germany	River	N/A	intertidal	1995.5	fibers, fragments, spheres, pellets	Fragments (51% for 630–5000 µm)	.063–.2 mm, .2–.63 mm, .63–5 mm	.2–.63 mm	Sewage treatment plants, plastic processing industry,	Klein et al., 2015
Yangtze River, China	Reservoir river	high energy (center of stream)	benthic sedim	162.5	Fiber, fragment, pellet,film and styrofoam.	fibers (33.9% to 100%)	<0.5 mm, 0.5–1 mm, 1–2mm,2–3 mm,3–4 mm,4–5 mm	<0.5 mm	industrial and household sewage, wastewater treatmentplant, garbage dumping, fishery, and agricultural	Di & Wang, 2018
Lake Ontario River tributaries	nearshore, tributary, and beach depositional sediments	varying energy dynamics between sample sites, sediment size	benthic, nearshore, beach sediment	760	Fibers, fragments, beads	Fragments	<2mm and >2mm	<2mm	Harbors, sewage and stormwater	Ballent, et. Al., 2016
(20)Urban wetlands in the Greater Melbourne Region, Victoria, Australia	wetland		inlet, middle, and outlet of wetlands with separate catchments	46	Fibers, fragments, beads	Fragments (68.5%)	N/A	N/A	industrial, stormwater, larger plastic items	Townsend et al., 2019
N. Gulf of Mexico (Mobile Bay, AL)	estuary	sand	intertidal	N/A	hard, film, foam, strand	hard plastics (47.8%)	0.2-5 mm	0.2 to 1 mm	Land based debris	Wessel et al 2016
Hangzhou Bay, China	salt marsh	low energy dynamic of salt marsh	benthic sediment	264	fibers, fragments, pellets, films	fibers (63%)	<.3 mm,.3–.5 mm, .5–.7 mm, .7–1mm.	.3–.5 mm	industrial, aquaculture	Li et al 2020
Changjiang Estuary, China	estuary	fine grain size	benthic sediment of estuary	180	fibers, fragments, pellets	fibers (93%)	<1 mm, 1-5 mm	<1 mm	Sewage treatment plants	Peng, et. Al., 2016
Vitoria Bay, Brazil	estuary	N/A	benthic sediment of estuary	63.3333333	fibers & fragments	fibers (77%)	N/A	N/A	fishing lines, harbor	Baptista Neto et al 2019
Bizerte Lagoon, Tunisia	Lagoon bottom sediment	N/A	shoreline sediment	7960	Fibers, fragments	fibers	0.3- 5 mm	Fibers: 1.39 ± 0.27; Fragments: 0.51 ± 0.19 mm	Cities discharge, fishing activity, industrial	Abidli, et. Al., 2017
Venice lagoon, Italy	Lagoon sediment	varying energy dynamics between sample sites, sediment size: 8 sites composed of mud, 2 sites composed of sand	benthic sediment of lagoon	1423.5	Fibers, fragments, films, pellets	Fragments (86%)	N/A	.03–.5 mm	aquaculture farms, plastic industries, city centers, freshwater runnoff	Vianello et al 2012
Great Lakes, Gulf of Mexico, Long Island Sound, Atlantic Ocean, Mississippi River	bottom sediment	varying energy dynamics between sample sites, sediment size	dredged and undredged harbors and channels	1636	fibers, fragments, spheres, foams, films	fragments	N/A	N/A	industrial, stormwater, wastewater, fishing, harbors, agriculture	Wilkens, et. Al., 2019
Belgium Harbor	(subtidal) mouths of coastal harbors	N/A	benthic sediment of harbor	166.7	fibers, granules, plastic films, PS spheres	fibers (59%)	N/A	N/A	harbors, plastic industries	Claessens et al., 2011
Continental Shelf, Belgium	21 km offshore	N/A	benthic sediment	97.2	fibers, granules, plastic films, PS spheres	fibers (59%)	N/A	N/A	harbors, plastic industries	Claessens et al., 2011
Waste Water Treatment Plants, Ireland	treated sewege sludge	>212µm>63 µm>45µm>	Waste Water Treatment Plants	9790.5	fibers, fragments, films, spheres, other	fibers (78.5%)	.25–.4 mm, .4–.6 mm, .6–1 mm, 1–4 mm	.25–.4 mm	industrial, stormwater, landfill	Mahon, A. M. (2017)
Elkhorn Slough	estuarine sediment		shoreline sediment	1602	Fibers, Fragments	fragments (89.5%)	.004-2.3mm	.04-.07 mm	Harbor, agriculture	current study